

Research Article

Identification of Chemical Components of Qi-Fu-Yin and Its Prototype Components and Metabolites in Rat Plasma and Cerebrospinal Fluid via UPLC-Q-TOF-MS

Hengyu Li ¹, Hongwei Zhao,¹ Yong Yang,¹ Dongmei Qi,¹ Xiaorui Cheng ¹,
and Jiafeng Wang ²

¹Innovative Institute of Chinese Medicine and Pharmacy, Shandong University of Traditional Chinese Medicine, Jinan 250355, China

²College of Traditional Chinese Medicine, Shandong University of Traditional Chinese Medicine, Jinan 250355, China

Correspondence should be addressed to Xiaorui Cheng; cxr916@163.com and Jiafeng Wang; wjfeng2000@126.com

Received 3 October 2021; Revised 11 December 2021; Accepted 14 December 2021; Published 28 December 2021

Academic Editor: Yanting Song

Copyright © 2021 Hengyu Li et al. This is an open access article distributed under the Creative Commons Attribution License, which permits unrestricted use, distribution, and reproduction in any medium, provided the original work is properly cited.

Qi-Fu-Yin, a traditional Chinese medicine formula, has been used to treat Alzheimer's disease (AD, a neurodegenerative disorder) in clinical setting. In this study, the chemical components of Qi-Fu-Yin and its prototype components and metabolites in rat plasma and cerebrospinal fluid, after oral administration, were preliminarily characterized via ultrahigh-performance liquid chromatography coupled with quadrupole time-of-flight tandem mass spectrometry (UPLC-Q-TOF-MS). A total of 180 compounds, including saponins, flavonoids, organic acids, sucrose esters, oligosaccharide esters, phthalides, phenylethanoid glycosides, alkaloids, xanthenes, terpene lactones, ionones, and iridoid glycoside, were tentatively characterized. For the first time, 51 prototypical components and 26 metabolites, including saponins, phthalides, flavonoids, sucrose esters, organic acids, alkaloids, ionones, terpene lactones, iridoid glycoside, and their derivatives, have been tentatively identified in the plasma. Furthermore, 10 prototypical components (including butylidenephthalide, butylphthalide, 20(S)-ginsenoside Rh₁, 20(R)-ginsenoside Rh₁, and zingibroside R₁) and 6 metabolites were preliminarily characterized in cerebrospinal fluid. These results were beneficial to the discovery of the active components of Qi-Fu-Yin anti-AD.

1. Introduction

Traditional Chinese medicine (TCM) plays a vital role in the treatment of various complex chronic diseases owing to the synergistic effects of the formulations and has, accordingly, garnered increasing attention worldwide [1, 2]. Qi-Fu-Yin, a TCM prescription, was first recorded in the book *Jingyue Encyclopedia* written by Jingyue Zhang during the Ming Dynasty. It is composed of seven herbs—Ginseng Radix et Rhizoma (GRR), Rehmanniae Radix Preparata (RRP), Angelicae Sinensis Radix (ASR), Atractylodis Macrocephala Rhizoma Preparata (ARP), Glycyrrhizae Radix et Rhizoma Preparata cum Melle (GRP), Ziziphi Spinosae Semen (ZSS), and Polygalae Radix Preparata (PRP)—in a ratio of 6:9:9:5:3:6:5 [3]. Qi-Fu-Yin has shown significant effects on

Alzheimer's disease (AD) in clinical studies [4, 5]. Owing to its remarkable therapeutic effects and pharmacological activities, Qi-Fu-Yin has attracted the attention of various researchers. Previous studies showed that Qi-Fu-Yin improves the learning ability and memory of rats injected with advanced glycation end products [6, 7] or β -amyloid protein [8, 9]. Furthermore, 154 chemical components were unambiguously identified or tentatively characterized in Qi-Fu-Yin using ultrahigh-performance liquid chromatography coupled with quadrupole time-of-flight tandem mass spectrometry (UHPLC-Q-TOF-MS) [10]. However, it remains unknown which components are absorbed into the plasma and brain after oral administration of Qi-Fu-Yin, which hinders the elucidation of its potentially bioactive constituents and the underlying action mechanisms.

AD is a neurodegenerative disease characterized by the deposition of $A\beta$ and the formation of neurofibrillary tangles in the brain [11]. The ingredients absorbed into blood and that reach a certain concentration can reportedly exert pharmacodynamic effects [12]. The blood-brain barrier (BBB) allows different components to reach the brain and prevents harmful substances from entering the brain. Drugs passing through the BBB can play important roles in brain diseases [13]. Some biotransformed metabolites possess substantial bioactivities and can act as active components [14]. Thus, it is essential to detect components absorbed into blood and elucidate their metabolic profile, which could reveal the pharmacologically active substances and provide potential resources for discovering new drugs from TCM. In this study, a three-step approach based on UHPLC-Q-TOF-MS was implemented to analyze the multicomponent metabolic profiles of Qi-Fu-Yin in rat plasma and cerebrospinal fluid. First, the Qi-Fu-Yin in vitro chemical component database was established by consulting literature on Qi-Fu-Yin and its seven constituent herbs. The components in vitro were identified by their corresponding MS/MS fragment ions in standard solutions and databases. Second, the database of the prototype components was established to characterize the prototypical components in rat plasma and cerebrospinal fluid after oral administration of Qi-Fu-Yin. Under the same LC-MS conditions, the prototype components were identified by comparing the standard solutions, extracts, control, and administered biological samples in parallel. Finally, according to the metabolic pathway and secondary mass spectrometry data of prototype components reported in the literature, the metabolites of Qi-Fu-Yin in plasma and cerebrospinal fluid were tentatively characterized (Figure 1).

2. Materials and Methods

2.1. Materials and Reagents. GRR, RRP, ASR, ARP, and GRP were purchased from Anxing Traditional Chinese Medicine Co., Ltd. (Anguo, China); ZSS and PRP were purchased from Juyatong Co., Ltd. (Anguo, China); reference standards of ferulic acid, liquiritin, spinosin, acteoside, 3,6'-disinapoyl sucrose, ginsenoside Rg₁ (G-Rg₁), ginsenoside Re (G-Re), ginsenoside Rb₁ (G-Rb₁), tenuifolin, and glycyrrhizic acid were purchased from the National Institute for Food and Drug Control (Beijing, China). Acetonitrile and formic acid were of HPLC grade (Fisher, Carlsbad, CA, USA). Deionized water was prepared using a Milli-Q purification system (Millipore, Bedford, MA, USA). Sodium formate was purchased from Waters (Milford, MA, USA).

2.2. Preparation of Samples of Qi-Fu-Yin and the Seven Herbs. Qi-Fu-Yin was prepared in the laboratory according to the prescribed protocol [3]. Dried pieces of GRR, RRP, ASR, ARP, GRP, ZSS (crushed), and PRP were accurately weighed and immersed in 9 times amount of water for 30 min; then, the samples were serially decocted with 9 times and 7 times amount of water. After mixing and filtering, the extracts were concentrated to a small volume and lyophilized. An

appropriate amount of the lyophilized powder was accurately weighed, dissolved in ultrapure water (equivalent to 50 mg crude drug per mL) in a 25 mL volumetric flask, and mixed evenly via ultrasonication for 30 min. Then, the extracts were centrifuged at 13000 rpm and 4°C for 10 min and filtered through a 0.22 μ m membrane. The seven herb samples of Qi-Fu-Yin were prepared in the same manner as the prescribed method.

2.3. Animals and Drug Administration. Male SD rats, weighing 200 ± 20 g, were purchased from Beijing Wei Tong Li Hua Experimental Animal Technology Co., Ltd. (Beijing, China). All animal procedures were approved by the Shandong University of Traditional Chinese Medicine Institutional Animal Experimentation Committee (SDUTCM20210119001). All rats were housed at an ambient temperature of $20 \pm 1^\circ\text{C}$ with a 12 h light/dark cycle and fed a standard diet and water ad libitum for 3 days before the experiment. The rats were then divided into a control group (orally administered deionized water) and a Qi-Fu-Yin group (orally administered Qi-Fu-Yin) ($n = 12$). To detect the prototype components and metabolites of Qi-Fu-Yin in the rat plasma and cerebrospinal fluid, an 8-fold clinical dosage (1.72 g crude drug per mL, 10 mL per kg, twice daily) was selected as the oral dose [6, 7]. All groups received intragastric administration twice daily for three consecutive days. Before the experiments, the animals fasted for 12 h, with free access to water.

2.4. Biological Sample Collection and Preparation. After the last intragastric administration, 500 μ L aliquots of serial blood samples were collected from the postorbital venous plexus vein of each rat at 0.5, 1.0, 2, and 4 h. Then, approximately 100 μ L of cerebrospinal fluid from each rat was collected at 4 h via percutaneous puncture of the cerebellar medulla cistern [15]. The biological samples collected in heparinized polythene tubes were centrifuged at 3000 rpm at 4°C for 15 min. Subsequently, the supernatant was transferred into new tubes and immediately stored at -80°C before preliminary treatment.

After unfreezing the biological samples in an ice-water mixture, plasma or cerebrospinal fluid was mixed at four different times to enrich the biological samples of each group. To each tube containing 1 mL of plasma or cerebrospinal fluid, 4 mL of methanol was added. The mixture was then vortexed for 2 min and centrifuged at 13000 rpm and 4°C for 10 min. Subsequently, the supernatant was transferred to another tube and dried using sanitary nitrogen gas at room temperature. Then, the residue was redissolved in 100 μ L of 30% methanol, vortexed for 2 min, and centrifuged at 13000 rpm and 4°C for 10 min.

2.5. UHPLC-Q-TOF-MS Analysis. An ultrahigh-performance liquid chromatography system (ACQUITY H-Class, Waters, Milford, MA, USA) coupled with a Q-TOF (Impact II, Bruker, Bremen, Germany) high-definition mass spectrometer in electrospray ionization mode was used for the

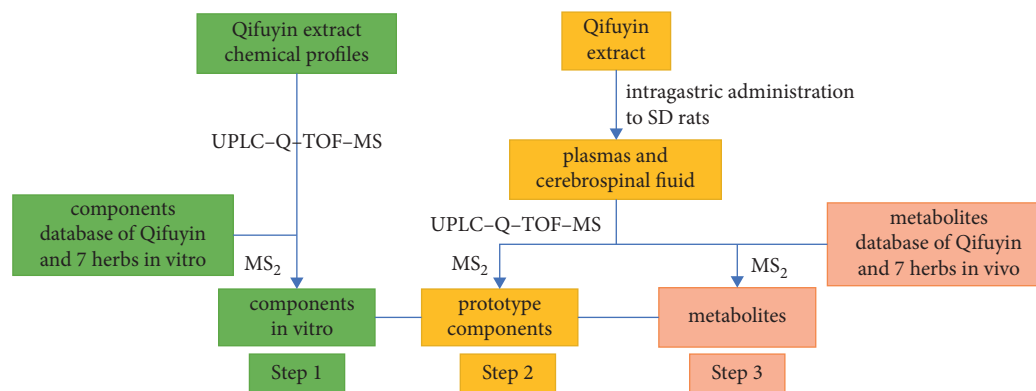


FIGURE 1: Research strategy for identifying the chemical components in Qi-Fu-Yin, in vitro and in vivo, via UPLC-Q-TOF-MS.

chromatographic and mass spectral analyses of all samples. An AMT Halo-C18 column (100 mm × 2.1 mm, 2.7 μm) with a column temperature of 30°C was selected as the separation system. The mobile phase consisted of eluent A (0.1% formic acid in water, v/v) and eluent B (acetonitrile), with a flow rate of 0.30 mL/min. These phases were delivered using a gradient program as follows: 8% B from 0 to 5 min, 8–17% from 5 to 15 min, 17–23% B from 15 to 27 min, 23–35% B from 27 to 43 min, 35–70% B from 43 to 51 min, 70–100% B from 51 to 55 min, and 100% B from 55 to 60 min.

The mass spectra operating parameters were set as follows: capillary voltage of 3.5 kV (ESI+) or −3.0 kV (ESI−), source temperature of 220°C, drying temperature of 220°C, and drying gas flow of 8 L/min. The collision energy was set to range from 35–75 V for MS/MS acquisition. To ensure mass accuracy and reproducibility, the mass spectrometer was calibrated over a range of 50–1500 Da using a sodium formate solution. All data were processed using Compass Data Analysis™ (V4.4, Bruker, Bremen, Germany).

3. Results

3.1. In Vitro Chemical Characterization of Qi-Fu-Yin. The base peak chromatograms (BPCs) of Qi-Fu-Yin in the positive and negative ion modes are shown in Figure S1. A total of 180 compounds, including 59 triterpene saponins, 26 flavonoids, 17 organic acids, 16 sucrose esters, 14 oligosaccharide esters, 13 phthalides, 12 phenylethanoid glycosides, 9 alkaloids, 6 xanthenes, 3 terpene lactones, 3 ionones, and 2 iridoid glycosides (Table 1), were identified. Twelve compounds were unambiguously identified via comparison with the standard solutions. The structures of other compounds were tentatively characterized based on their retention times, fragmentation pathways, and MS/MS spectra, by referring to the literature.

3.1.1. GRR. Triterpene saponins are the main components of GRR [45]. Ginsenosides can be divided into protopanaxatriol (PPT), protopanaxadiol (PPD), and oleanolic acid (OA) according to their mother skeleton. The diagnostic ions at m/z 475.38, 459.38, and 455.35 corresponded to the PPT, PPD, and OA-type aglycones, respectively. Some

special PPT-type ginsenosides were detected at m/z 457.37 owing to dehydration between the 20(21) or 20(22) bonds (Table 1). Continuous or simultaneous loss of different types of glycosyl moieties is another characteristic fragment distribution of ginsenosides. The 132, 146, 162, and 176 Da values indicated the presence of an Ara or Xyl, Rha, Glc, and GlcA glycosyl moiety, respectively. Based on the fragmentation rules, 28 saponins were identified.

Compound 142 produced the adduct ion $[M + \text{COOH}]^-$ (m/z 1123.5918) and deprotonated molecular ion $[M - \text{H}]^-$ (m/z 1077.5854), indicating a molecular formula of $\text{C}_{53}\text{H}_{90}\text{O}_{22}$. Diagnostic ions at m/z 915.5348, 783.4945, 621.4401, and 459.3809 revealed that it was a PPD-type ginsenoside with continuous or simultaneous elimination of Glc and Ara moieties. Thus, compound 142 was assigned to ginsenoside Rc (Table 1). Analogously, PPT-type compounds 79, 84, 88, 104, 118, 123, 131–133, 136, and 137 and PPD-type compounds 139, 142, 144, 145, 149, 170, 174, 176, 178, and 179 were also preliminarily characterized according to their fragmentation pathways and retention times (Table 1). Compounds 158, 164, 165, and 168 had characteristic fragments at m/z 457.37 and were characterized as special PPT-type ginsenosides (Table 1).

Compound 141 only produced a deprotonated molecular ion $[M - \text{H}]^-$ and diagnostic ions at m/z 455.3527, which indicated that it was an OA-type ginsenoside. Fragmentation ions at m/z 793.4382, 731.4392, 613.3755, and 569.3857 indicated the continuous or simultaneous loss of Glc, GlcA, and CO_2 . Similarly, compounds 148 and 169 were tentatively assigned (Table 1).

3.1.2. RRP. Iridoid glycosides are considered the main components of RRP. The negative ion mode was selected to characterize the RRP components because the fragmentation pathway of glycosyl was easier to detect in the negative ion mode (Figure S1). According to the fragmentation rules, 12 phenylethanoid glycosides, 2 iridoid glycosides, 3 ionone glycosides, and 1 organic acid were identified.

The loss of acyl residues is a characteristic fragmentation pattern of phenylethanoid glycosides. Compound 53 produced a deprotonated molecular ion $[M - \text{H}]^-$ (m/z 623.1989) in the negative ion mode, which indicated a

TABLE 1: Characterization of chemical components in Qi-Fu-Yin.

No.	t_R (min)	Name	Classification	Formula	Theoretical mass (Da)	Measured mass (Da)	Error (ppm)	Precursor ions	Main MS/MS fragment ions	Source	Ref.
1	0.99	Citric acid*	Organic acids	$C_6H_8O_7$	191.0197	191.0201	2.1	$[M-H]^-$	129.0196, 111.009	ZSS, ASR, ARP	[16]
2	1.37	Geniposidic acid	Iridoid glycoside	$C_{16}H_{22}O_{10}$	373.1140	373.1143	0.8	$[M-H]^-$	211.0605, 193.0497, 167.0703, 149.0595, 123.0437	RRP	[10]
3	1.85	Decaffeoylactoside*	Phenylethanoid glycosides	$C_{20}H_{30}O_{12}$	461.1664	461.1669	1.1	$[M-H]^-$	375.1314, 315.1314, 297.0980, 135.0452	RRP	[17]
4	1.95	Mussaenosidic acid*	Iridoid glycoside	$C_{16}H_{24}O_{10}$	375.1297	375.1299	0.5	$[M-H]^-$	213.0778, 169.0873, 151.0766	RRP	[18]
5	2.05	5-Caffeoylquinic acid*	Organic acids	$C_{16}H_{18}O_9$	353.0878	353.0878	0.0	$[M-H]^-$	191.0563, 179.0352, 161.0245, 155.0350, 111.0088	ASR	[19]
6	2.34	3-Caffeoylquinic amide*	Organic acids	$C_{16}H_{19}NO_8$	354.1183	354.1178	-1.5	$[M+H]^+$	192.0650, 174.0545, 146.0597	ASR	[10]
7	2.82	Ferulic acid hexoside*	Organic acids	$C_{16}H_{20}O_9$	355.1035	355.1042	2.0	$[M-H]^-$	193.0509, 149.0610, 178.0271, 134.0375	ASR	[20]
8	3.01	3-Caffeoylquinic amide isomer*	Organic acids	$C_{16}H_{19}NO_8$	354.1183	354.1177	-1.8	$[M+H]^+$	192.0650, 174.0545, 146.0597	ZSS	[10]
9	3.03	Hydroxybenzoic acid*	Organic acids	$C_7H_6O_3$	137.0244	137.0244	0.0	$[M-H]^-$	136.0170, 108.0215	ZSS	[16]
10	3.21	p-Hydroxybenzyl malonic acid*	Organic acids	$C_{10}H_{10}O_5$	209.0455	209.0456	0.5	$[M-H]^-$	419.0982, 165.0562, 121.0662	GRP	[21]
11	3.34	Sanjoinine IB*	Alkaloids	$C_{19}H_{21}NO_4$	328.1543	328.1534	-2.7	$[M+H]^+$	265.0855, 251.0665, 237.0902, 223.0712	ZSS	[22]
12	3.53	Magnocurarine*	Alkaloids	$C_{19}H_{24}NO_3+$	314.1751	314.1748	-1.0	$[M]^+$	269.1179, 237.0897, 209.0947, 175.0744, 107.0491	ZSS	[22]
13	3.69	Chlorogenic acid	Organic acids	$C_{16}H_{18}O_9$	353.0878	353.0885	2.0	$[M-H]^-$	191.0563, 127.0404	ASR	[20]
14	4.26	Sibiricoside A5	Sucrose esters	$C_{22}H_{30}O_{14}$	517.1563	517.1568	1.0	$[M-H]^-$	341.1097, 193.0512, 175.0404, 160.0169	PRP	[23]
15	4.55	4-Caffeoylquinic acid	Organic acids	$C_{16}H_{18}O_9$	353.0878	353.0883	1.4	$[M-H]^-$	191.0562, 179.0350, 173.0457, 161.0243, 111.0453, 93.0346	ASR	[10]
16	4.74	Vanillic acid	Organic acids	$C_8H_8O_4$	167.0350	167.0351	0.6	$[M-H]^-$	123.0452	ASR	[24]
17	5.32	Sibiricoside A6*	Sucrose esters	$C_{23}H_{32}O_{15}$	547.1668	547.1678	1.8	$[M-H]^-$	367.1034, 341.1094, 223.0616, 205.0508, 190.0274	PRP	[25, 26]
18	5.54	Sanjoinine K	Alkaloids	$C_{17}H_{19}NO_3$	286.1438	286.1431	-2.3	$[M+H]^+$	269.1154, 237.0905, 175.0751, 107.0492	ZSS	[16]
19	5.90	Ferulic acid hexoside isomer*	Organic acids	$C_{16}H_{20}O_9$	355.1035	355.1041	1.7	$[M-H]^-$	193.0512, 149.0610, 178.0273, 134.0376	ASR	[20]
20	5.99	Darendoside B*	Phenylethanoid glycosides	$C_{21}H_{32}O_{12}$	475.1821	475.1830	1.9	$[M-H]^-$	329.1228, 311.1144, 161.0459, 113.0247	RRP	[27]
21	6.18	Liquiritigenin-7,4'-di-O- glucoside	Flavonoids	$C_{27}H_{32}O_{14}$	579.1719	579.1733	2.4	$[M-H]^-$	417.1212, 255.0669, 135.0086	GRP	[28]
22	6.38	Caffeic acid	Organic acids	$C_9H_8O_4$	179.0350	179.0352	1.1	$[M-H]^-$	151.0459, 135.0499	ASR	[10]
23	7.47	Magnoflorine	Alkaloids	$C_{20}H_{23}NO_4+$	342.1700	342.1689	-3.2	$[M+H]^+$	297.1113, 282.0876, 265.0848	ZSS	[16]
24	9.46	Feruloylquinic acid*	Organic acids	$C_{17}H_{20}O_9$	367.1035	367.1043	2.2	$[M-H]^-$	191.0563, 173.0461, 111.0453, 93.035	ASR	[20]
25	9.82	Lotusine*	Alkaloids	$C_{19}H_{24}NO_3+$	314.1751	314.1752	0.3	$[M]^+$	269.1162, 237.0912, 209.0949, 107.0485	ZSS	[22]

TABLE 1: Continued.

No.	t_R (min)	Name	Classification	Formula	Theoretical mass (Da)	Measured mass (Da)	Error (ppm)	Precursor ions	Main MS/MS fragment ions	Source	Ref.
26	9.94	Feruloylquinic acid isomer*	Organic acids	$C_{17}H_{20}O_9$	367.1035	367.1034	-0.3	[M-H] ⁻	191.0564, 173.0457, 111.0450, 93.0347	ASR	[20]
27	10.04	Sibiricoside A1	Sucrose esters	$C_{23}H_{32}O_{15}$	547.1668	547.1676	1.5	[M-H] ⁻	367.1040, 223.016, 190.0275	PRP	[10, 23]
28	10.23	Vicenin II	Flavonoids	$C_{27}H_{30}O_{15}$	593.1512	593.1522	1.7	[M-H] ⁻	503.1200, 473.1098, 383.0780, 353.0674, 325.0931,	GRP, ZSS	[16, 22]
29	10.43	Ferulic acid isomer**	Organic acids	$C_{10}H_{10}O_4$	193.0506	193.0506	0.0	[M-H] ⁻	149.0243, 121.0298	PRP	[23]
30	10.81	Lancerin	Xanthones	$C_{19}H_{18}O_{10}$	405.0827	405.0833	1.5	[M-H] ⁻	285.0410, 257.0456	RRP	[10, 17]
31	11.30	Rehmannioside A/B	Ionones	$C_{19}H_{34}O_8$	435.2239	435.2246	1.6	[M+COOH] ⁻	389.2223, 179.0591	RRP	[10, 17]
32	11.49	Ferulic acid	Organic acids	$C_{10}H_{10}O_4$	193.0506	193.0507	0.5	[M-H] ⁻	178.0272, 149.0609, 134.0369	ASR	[20]
33	11.97	Lancerin isomer*	Xanthones	$C_{19}H_{18}O_{10}$	405.0827	405.0833	1.5	[M-H] ⁻	285.0413, 315.0518, 257.0458	PRP	[10]
34	12.14	Caaverine*	Alkaloids	$C_{17}H_{17}NO_2$	268.1332	268.1321	-4.1	[M-H] ⁻	251.1014, 219.0829, 209.0933, 191.0862	ZSS	[22]
35	12.45	Sibiricaxanthone A/B	Xanthones	$C_{24}H_{26}O_{14}$	537.1250	537.1258	1.5	[M-H] ⁻	405.0832, 387.0730, 327.0524, 315.0514, 297.0412, 285.0410, 267.0303, 243.0302	PRP	[29]
36	12.45	Echinacoside	Phenylethanoid glycosides	$C_{35}H_{46}O_{20}$	785.2510	785.2520	1.3	[M-H] ⁻	623.2201, 461.1663, 161.0245	RRP	[30]
37	12.74	Schaftoside	Flavonoids	$C_{26}H_{28}O_{14}$	563.1406	563.1408	0.4	[M-H] ⁻	353.0674, 443.0992, 473.1098, 383.0778, 503.1197, 425.0877, 413.0882	GRP	[31]
38	13.12	Sibiricoside A2	Sucrose esters	$C_{24}H_{34}O_{15}$	561.1825	561.1832	1.2	[M-H] ⁻	607.1888, 323.0991, 237.0771	PRP	[10]
39	13.41	Rehmannioside A/B	Ionones	$C_{19}H_{34}O_8$	435.2239	435.2239	0.0	[M+COOH] ⁻	389.2223, 179.0572	RRP	[29]
40	13.79	Liquiritin	Flavonoids	$C_{21}H_{22}O_9$	417.1191	417.1194	0.7	[M-H] ⁻	255.0665, 135.0089, 119.0504	GRP	[31]
41	14.08	Polygalaxanthone III	Xanthones	$C_{25}H_{28}O_{15}$	567.1355	567.1361	1.1	[M-H] ⁻	447.0945, 435.0932, 417.0839, 357.0621, 345.0620, 327.0518, 315.0515, 297.0408	PRP	[10]
42	14.27	Ionoside E*	Phenylethanoid glycosides	$C_{35}H_{46}O_{19}$	769.2561	769.2568	0.9	[M-H] ⁻	623.2197, 605.2092, 549.1662, 427.1069, 323.0996, 179.0561	RRP	[27]
43	14.37	Liquiritin apioside	Flavonoids	$C_{26}H_{30}O_{13}$	549.1614	549.1616	0.4	[M-H] ⁻	255.06581, 135.00719, 119.04859, 417.11804	GRP	[31]
45	14.47	Asimilobine*	Alkaloids	$C_{17}H_{17}NO_2$	268.1332	268.1324	-3.0	[M-H] ⁻	251.1064, 219.0809, 201.0722, 191.0858, 179.0855	ZSS	[22]
44	14.47	Polygalaxanthone XI*	Xanthones	$C_{25}H_{28}O_{15}$	567.1355	567.1366	1.9	[M-H] ⁻	345.0619, 315.0511	PRP	[32]
46	14.56	Ionoside A1/ionoside A2	Phenylethanoid glycosides	$C_{36}H_{48}O_{20}$	799.2666	799.2672	0.8	[M-H] ⁻	623.2199, 605.2092, 461.1663, 315.1110, 193.0509, 175.0403	RRP	[30]
47	14.85	Spinosin	Flavonoids	$C_{28}H_{32}O_{15}$	607.1668	607.1674	1.0	[M-H] ⁻	487.1252, 445.1144, 427.1039, 367.0823, 337.0722, 307.0614	ZSS	[16]
48	15.33	Swertisin	Flavonoids	$C_{22}H_{22}O_{10}$	445.1140	445.1147	1.6	[M-H] ⁻	355.0839, 325.0721, 297.0409	ZSS	[16]
49	15.33	Isoviolanthin/violanthin*	Flavonoids	$C_{27}H_{30}O_{14}$	577.1563	577.1572	1.6	[M-H] ⁻	383.0777, 353.0670, 413.08783, 457.1145, 487.1248	GRP	[31]
50	15.43	Tenuifolioside B	Sucrose esters	$C_{30}H_{36}O_{17}$	667.1880	667.1894	2.1	[M-H] ⁻	461.1312, 205.0510, 190.0274, 137.0247, 281.0674	PRP	[23]

TABLE 1: Continued.

No.	t_R (min)	Name	Classification	Formula	Theoretical mass (Da)	Measured mass (Da)	Error (ppm)	Precursor ions	Main MS/MS fragment ions	Source	Ref.
51	15.52	Sibiricoside A4*	Sucrose esters	C ₃₄ H ₄₂ O ₁₉	753.2248	753.2254	0.8	[M - H] ⁻	547.1678, 529.1574, 461.1306, 367.1041, 223.0615, 205.0509, 190.0274	PRP	[29]
52	15.71	Tenuifoliside 638*	Sucrose esters	C ₂₉ H ₃₄ O ₁₆	637.1774	637.1773	-0.2	[M - H] ⁻	461.1309, 443.1208, 175.0402	PRP	[29]
53	16.48	Acteoside	Phenylethanoid glycosides	C ₂₉ H ₃₆ O ₁₅	623.1981	623.1989	1.3	[M - H] ⁻	461.1667, 443.1555, 315.1083, 179.0349, 161.0243	RRP	[30]
54	17.06	6'''-Vanilloylspinosin*	Flavonoids	C ₃₆ H ₃₈ O ₁₈	757.1985	757.1993	1.1	[M - H] ⁻	637.1556, 607.1694, 445.1143, 427.1038, 367.0827, 307.0621	ZSS	[22]
55	17.25	Senkyunolide I	Phthalides	C ₁₂ H ₁₆ O ₄	207.1015	207.1009	-2.9	[M + H - H ₂ O] ⁺	189.0822, 161.0906, 147.0752	ASR	[33]
56	17.44	Jionoside B1/Jionoside B2	Phenylethanoid glycosides	C ₃₇ H ₅₀ O ₂₀	813.2823	813.2834	1.4	[M - H] ⁻	637.2359, 619.2254, 491.1780, 193.0507, 175.0402, 160.0167	RRP	[16]
57	17.63	6'''-p-Hydroxyl- benzoyspinosin*	Flavonoids	C ₃₅ H ₃₆ O ₁₇	727.1880	727.1879	-0.1	[M - H] ⁻	607.1616, 445.1149, 427.1038, 325.0719, 307.0617	ZSS	[16]
58	17.73	Isoacteoside	Phenylethanoid glycosides	C ₂₉ H ₃₆ O ₁₅	623.1981	623.1990	1.4	[M - H] ⁻	461.1670, 477.1405, 315.1096, 179.0351, 161.0245	RRP	[30]
59	18.69	Tenuifoliside A isomer*	Sucrose esters	C ₃₁ H ₃₈ O ₁₇	681.2036	681.2044	1.2	[M - H] ⁻	443.1208, 281.0672, 237.0774, 223.0616, 205.0510, 137.0246	PRP	[23]
60	18.78	Senkyunolide H	Phthalides	C ₁₂ H ₁₆ O ₄	207.1015	207.1008	-3.4	[M + H - H ₂ O] ⁺	189.0812, 161.0938, 147.0689	ASR	[33]
61	18.98	3,6'-Disinapoyl sucrose	Sucrose esters	C ₃₄ H ₄₂ O ₁₉	753.2248	753.2249	0.1	[M - H] ⁻	547.1670, 529.1568, 367.1038, 265.0720, 223.0612, 205.0506, 190.0271	PRP	[10]
62	19.02	Nornuciferine*	Alkaloids	C ₁₈ H ₁₉ NO ₂	282.1489	282.1481	-2.7	[M + H] ⁺	265.1214, 250.0979, 121.0280	ZSS	[22]
63	19.05	6'''-Sinapoyl spinosin	Flavonoids	C ₃₉ H ₄₂ O ₁₉	815.2393	815.2379	-1.7	[M + H] ⁺	429.1181, 411.1037, 369.1162, 327.0855, 207.0647, 351.0833, 297.0750, 175.0385	ZSS	[16]
64	19.21	6'''-Dihydrophaseoylspinosin*	Flavonoids	C ₄₃ H ₅₂ O ₁₉	873.3176	873.3158	-2.0	[M + H] ⁺	855.2986, 447.1263, 429.1140, 411.1057, 393.0969, 381.0947, 351.0846, 327.0854, 297.0752, 247.1321	ZSS	[22]
65	19.56	3,4,5-Trimethoxycinnamic acid*	Organic acids	C ₁₂ H ₁₄ O ₅	237.0768	237.0770	0.8	[M - H] ⁻	193.0873, 108.0215	PRP	[34]
66	19.60	6'''-p-Coumaroyl spinosin	Flavonoids	C ₃₇ H ₃₈ O ₁₇	755.2182	755.2166	-2.1	[M + H] ⁺	429.1170, 411.1080, 351.0850, 327.0854, 147.0438, 635.1770, 381.0957, 297.0750	ZSS	[16]
67	19.66	Jionoside D	Phenylethanoid glycosides	C ₃₀ H ₃₈ O ₁₅	637.2138	637.2137	-0.2	[M - H] ⁻	161.0242, 461.1660, 267.0660, 175.0401	RRP	[10]
68	19.66	Arillanin A*	Sucrose esters	C ₃₃ H ₄₀ O ₁₈	723.2142	723.2149	1.0	[M - H] ⁻	547.1679, 265.0722, 223.0617, 205.0510, 175.0404, 160.0170	PRP	[32]
69	19.73	6'''-Feruloyl spinosin	Flavonoids	C ₃₈ H ₄₀ O ₁₈	785.2287	785.2263	-3.1	[M + H] ⁺	665.1891, 447.1275, 429.1168, 411.1068, 393.0957, 351.0852, 327.0853, 297.0750, 177.0542	ZSS	[10]
70	19.95	Tenuifoliside 652*	Sucrose esters	C ₃₀ H ₃₆ O ₁₆	651.1931	651.1942	1.7	[M - H] ⁻	443.1199, 281.0671, 207.0668, 175.0403, 137.0244	PRP	[29]

TABLE 1: Continued.

No.	t_R (min)	Name	Classification	Formula	Theoretical mass (Da)	Measured mass (Da)	Error (ppm)	Precursor ions	Main MS/MS fragment ions	Source	Ref.
71	20.81	Ononin*	Flavonoids	$C_{22}H_{22}O_9$	475.1246	475.1249	0.6	[M + COOH] ⁻	475.1249, 267.0664, 252.0429	GRP	[31]
72	21.00	Tenuifolioside 652 isomer*	Sucrose esters	$C_{30}H_{36}O_{16}$	651.1931	651.1941	1.5	[M - H] ⁻	443.1199, 205.0509, 190.0272, 175.0033, 121.0297	PRP	[29]
73	21.10	Isoliquiritin apioside	Flavonoids	$C_{26}H_{30}O_{13}$	549.1614	549.1620	1.1	[M - H] ⁻	255.0667, 135.0090, 119.0505, 417.1200	GRP	[10]
74	21.48	Isoliquiritin	Flavonoids	$C_{21}H_{22}O_9$	417.1191	417.1197	1.4	[M - H] ⁻	255.0666, 135.0089, 119.0404	GRP	[10]
75	21.77	Leucosceptoside A	Phenylethanoid glycosides	$C_{30}H_{38}O_{15}$	637.2138	637.2129	-1.4	[M - H] ⁻	461.1661, 175.0400, 265.0722, 161.0239	RRP	[30]
76	21.77	Tenuifolioside A	Sucrose esters	$C_{31}H_{38}O_{17}$	681.2036	681.2038	0.3	[M - H] ⁻	443.1203, 281.0671, 239.0564, 179.0352, 137.0245	PRP	[10]
77	22.06	Liquiritigenin	Flavonoids	$C_{15}H_{12}O_4$	255.0663	255.0665	0.8	[M - H] ⁻	135.0086, 119.0502	GRP	[31]
78	22.64	Neoisoliquiritin*	Flavonoids	$C_{21}H_{22}O_9$	417.1191	417.1197	1.4	[M - H] ⁻	255.0667, 135.0089, 119.0505	GRP	[28]
79	22.64	Notoginsenoside R1*	Saponins	$C_{47}H_{80}O_{18}$	977.5327	977.5334	0.7	[M + COOH] ⁻	931.5284, 637.4332, 475.3809	GRR	[35]
80	22.83	6'''(-)-Phaseoylspinosin*	Flavonoids	$C_{43}H_{50}O_{19}$	869.2874	869.2884	1.2	[M - H] ⁻	839.2765, 607.1683, 589.1575, 427.1045	ZSS	[22]
81	23.70	Tenuifolioside G	Oligosaccharide esters	$C_{66}H_{84}O_{38}$	1483.4568	1483.4582	0.9	[M - H] ⁻	1337.39795, 1295.38232, 1161.35095, 1119.34119, 997.30548, 851.27283, 753.22705, 631.18640, 452.31161, 307.08231, 175.03891, 163.03868, 145.02803	PRP	[10]
82	23.80	Senkyunolide D*	Phthalides	$C_{12}H_{14}O_4$	221.0819	221.0820	0.5	[M - H] ⁻	177.0921, 147.0450	ASR	[36]
83	23.80	Tenuifolioside M	Oligosaccharide esters	$C_{65}H_{82}O_{37}$	1453.4462	1453.4490	1.9	[M - H] ⁻	1307.3873, 1161.3532, 997.3064, 835.2514, 307.0824, 163.0385, 145.0280	PRP	[10]
84	24.48	Ginsenoside Rg1	Saponins	$C_{42}H_{72}O_{14}$	845.4904	845.4912	0.9	[M + COOH] ⁻	799.4877, 637.4342, 475.3809, 161.0458, 179.0565	GRR	[31]
85	24.67	Licorice glycoside B	Flavonoids	$C_{35}H_{36}O_{15}$	695.1981	695.1991	1.4	[M - H] ⁻	549.1634, 163.0409, 417.1202, 255.0665, 399.1099, 531.1523, 175.0403	GRP	[31]
86	24.77	Isomartynoside*	Phenylethanoid glycosides	$C_{31}H_{40}O_{15}$	651.2294	651.2303	1.4	[M - H] ⁻	505.1703, 475.1826, 193.0511, 175.0403, 160.017, 113.0245	RRP	[37]
87	24.77	Licorice glycoside A	Flavonoids	$C_{36}H_{38}O_{16}$	725.2087	725.2095	1.1	[M - H] ⁻	549.1639, 255.0668, 193.0508, 135.0086	GRP	[38]
88	24.86	Ginsenoside Re	Saponins	$C_{48}H_{82}O_{18}$	991.5483	991.5501	1.8	[M + COOH] ⁻	945.5442, 783.4916, 637.4329, 475.3793, 179.0562, 161.0457	GRR	[31]
89	26.11	Senkyunolide D isomer*	Phthalides	$C_{12}H_{14}O_4$	221.0819	221.0817	-0.9	[M - H] ⁻	177.0920, 147.0453	ASR	[36]
90	26.31	Tenuifolioside C	Sucrose esters	$C_{35}H_{44}O_{19}$	767.2404	767.2416	1.6	[M - H] ⁻	529.1567, 367.1038, 237.077, 223.0613, 205.0507, 190.0271, 122.33637, 107.73279,	PRP	[10]
91	26.69	Tenuifolioside T*	Oligosaccharide esters	$C_{56}H_{70}O_{32}$	1253.3777	1253.3792	1.2	[M - H] ⁻	955.2908, 647.1988, 451.1232, 307.0810, 287.0549, 257.0444	PRP	[23]

TABLE 1: Continued.

No.	t_R (min)	Name	Classification	Formula	Theoretical mass (Da)	Measured mass (Da)	Error (ppm)	Precursor ions	Main MS/MS fragment ions	Source	Ref.
92	26.88	Martynoside*	Phenylethanoid glycosides	$C_{31}H_{40}O_{15}$	651.2294	651.2299	0.8	[M - H] ⁻	505.172, 475.1829, 193.0508, 175.0403, 160.0169, 113.0244	RRP	[17]
93	26.90	(hydroxy benzoyl)-(hydroxy cinnamoyl)-trihydroxyphenyl sucrose	Sucrose esters	$C_{34}H_{42}O_{18}$	783.2353	783.2365	1.5	[M + COOH] ⁻	737.2325, 615.1934, 467.1415, 323.0980, 179.0547, 161.0458, 147.0453, 121.0296	PRP	[10]
94	27.75	Tenuifoliose L	Oligosaccharide esters	$C_{67}H_{84}O_{38}$	1495.4569	1495.4569	0.0	[M - H] ⁻	1349.3923, 1307.3988, 163.0410, 145.0294	PRP	[10]
95	28.14	Tenuifoliose K	Oligosaccharide esters	$C_{57}H_{70}O_{32}$	1265.3777	1265.3801	1.9	[M - H] ⁻	1119.3395, 1077.3346, 997.3037, 163.0403, 145.0294	PRP	[10]
96	29.00	Tenuifoliose C	Oligosaccharide esters	$C_{58}H_{72}O_{33}$	1295.3883	1295.3903	1.5	[M - H] ⁻	1173.3653, 1119.3401, 1077.3265, 997.3061, 145.0296, 175.0404	PRP	[10]
97	29.78	Amphibine D*	Alkaloids	$C_{36}H_{49}N_3O_5$	632.3806	632.3805	-0.2	[M + H] ⁺	289.1874, 148.1111	ZSS	[16]
98	30.35	Desacetylsenegasaponin B*	Saponins	$C_{57}H_{70}O_{32}$	1265.5808	1265.5831	1.8	[M - H] ⁻	455.3179, 425.3077	PRP	[29]
99	30.44	Uralsaponin C	Saponins	$C_{42}H_{64}O_{16}$	823.4122	823.4133	1.3	[M - H] ⁻	647.3829, 351.0580, 193.0357	GRP	[28]
100	30.44	Tenuifoliose I	Oligosaccharide esters	$C_{59}H_{72}O_{33}$	1307.3883	1307.3904	1.6	[M - H] ⁻	1161.3529, 1119.3479, 1101.3331, 997.3023, 631.1891, 163.0400, 145.0299	PRP	[10]
101	30.70	Aeginetic acid*	Ionones	$C_{15}H_{24}O_4$	267.1602	267.1610	3.0	[M - H] ⁻	223.1780, 205.1615, 178.9208, 153.0924	RRP	[39]
102	30.81	Methoxyl benzoyl-trimethoxyl cinnamoyl sucrose	Sucrose esters	$C_{32}H_{40}O_{17}$	741.2248	741.2255	0.9	[M + COOH] ⁻	237.0773, 151.0402	PRP	[10]
103	31.12	Tenuifoliose D	Oligosaccharide esters	$C_{60}H_{74}O_{34}$	1337.3989	1337.4007	1.3	[M - H] ⁻	1161.3546, 1119.3412, 1039.3161, 997.3030, 175.0404	PRP	[10]
104	31.41	Notoginsenoside R2	Saponins	$C_{41}H_{70}O_{13}$	815.4834	815.4834	0.0	[M + COOH] ⁻	769.4745, 637.4342, 475.3791, 161.0462	GRR	[40]
105	31.41	Tenuifoliose E*	Oligosaccharide esters	$C_{58}H_{72}O_{33}$	1295.3883	1295.3933	3.9	[M - H] ⁻	1173.3506, 1119.3442, 795.2398, 175.0404, 145.0300	PRP	[29]
106	31.79	Polygalasaponin XXIII*	Saponins	$C_{53}H_{82}O_{24}$	1101.5123	1101.5164	3.7	[M - H] ⁻	423.2925, 453.3029	PRP	[29]
107	32.08	Polygalasaponin XXVIII	Saponins	$C_{53}H_{84}O_{24}$	1103.5380	1103.5328	-4.7	[M - H] ⁻	455.3185, 425.3075	PRP	[23]
108	32.28	24-Hydroxyl-licorice-saponin A ₃	Saponins	$C_{48}H_{72}O_{22}$	999.4442	999.4488	4.6	[M - H] ⁻	837.3942, 351.0584, 193.0359	GRP	[10]
109	32.57	Tenuifoliose J*	Oligosaccharide esters	$C_{59}H_{72}O_{33}$	1307.3883	1307.3898	1.1	[M - H] ⁻	1161.3549, 1039.3096, 163.0408, 145.0304	PRP	[29, 32]
110	32.81	Butyridenephthalide	Phthalides	$C_{12}H_{12}O_2$	189.0910	189.0904	-3.2	[M + H] ⁺	171.0799, 161.0954, 143.0852, 117.0694	ASR	[20]
111	32.85	Senkyunolide F*	Phthalides	$C_{12}H_{14}O_3$	205.0870	205.0880	4.9	[M - H] ⁻	161.0975	ASR	[20]
112	32.92	Uralsaponin F	Saponins	$C_{44}H_{64}O_{19}$	895.3969	895.3995	2.9	[M - H] ⁻	719.3703, 351.0586, 193.0363	GRP	[31]
113	32.95	Onjisaponin TF	Saponins	$C_{59}H_{94}O_{28}$	1249.5859	1249.5880	1.7	[M - H] ⁻	1025.5362, 455.3185, 425.3077	PRP	[23]
114	33.05	Licorice saponin H2/K2*	Saponins	$C_{42}H_{62}O_{16}$	821.3965	821.3981	1.9	[M - H] ⁻	351.0583, 193.0364, 175.0255	GRP	[28, 41]
115	33.05	22-Hydroxyl-licorice-saponin G ₂	Saponins	$C_{42}H_{62}O_{18}$	853.3863	853.3882	2.2	[M - H] ⁻	677.3568, 351.0583, 193.0365	GRP	[28]

TABLE 1: Continued.

No.	t_R (min)	Name	Classification	Formula	Theoretical mass (Da)	Measured mass (Da)	Error (ppm)	Precursor ions	Main MS/MS fragment ions	Source	Ref.
116	33.22	Butylphthalide	Phthalides	$C_{12}H_{14}O_2$	191.1067	191.1062	-2.6	$[M+H]^+$	173.0959, 155.0842, 145.1008, 117.0698	ASR	[20]
117	33.34	Tenuifoliose B	Oligosaccharide esters	$C_{60}H_{74}O_{34}$	1337.3989	1337.4027	2.8	$[M-H]^-$	1161.3551, 1119.342, 1101.3324, 1039.3156, 175.0410, 145.0306	PRP	[10]
118	33.92	Ginsenoside Rf	Saponins	$C_{42}H_{72}O_{14}$	845.4904	845.4928	2.8	$[M+COOH]^-$	799.4880, 637.4349, 475.3820, 179.0574, 161.0466	GRR	[35]
119	33.92	Tenuifoliose H	Oligosaccharide esters	$C_{61}H_{74}O_{34}$	1349.3989	1349.4019	2.2	$[M-H]^-$	1307.3907, 1161.3503, 731.2194, 145.0304	PRP	[10]
120	34.40	Senkyunolide A	Phthalides	$C_{12}H_{16}O_2$	193.1223	193.1218	-2.6	$[M+H]^+$	147.1170, 175.1113, 137.0593	ASR	[20]
121	34.59	Tenuifoliose A	Oligosaccharide esters	$C_{62}H_{76}O_{35}$	1379.4094	1379.4131	2.7	$[M-H]^-$	1203.3649, 1161.3529, 175.041, 145.0303	PRP	[10]
122	35.08	Tenuifoliose N [*]	Oligosaccharide esters	$C_{63}H_{78}O_{36}$	1409.4200	1409.4234	2.4	$[M-H]^-$	1233.3879, 175.0410	PRP	[23]
123	35.37	Ginsenoside F5 [*]	Saponins	$C_{41}H_{70}O_{13}$	815.4834	815.4821	-1.6	$[M+COOH]^-$	769.4765, 637.4337, 475.3807	GRR	[42]
124	35.41	Licorice saponin A3	Saponins	$C_{48}H_{72}O_{21}$	983.4493	983.4518	2.5	$[M-H]^-$	821.3988, 645.3687, 351.0584, 193.0366	GRP	[31]
125	35.79	24-Hydroxyl-licorice-saponin E2	Saponins	$C_{42}H_{60}O_{17}$	835.3793	835.3785	-1.0	$[M-H]^-$	659.3446, 351.0582, 193.0362	GRP	[28]
126	35.84	Isoliquiritigenin ^{**}	Flavonoids	$C_{15}H_{12}O_4$	255.0663	255.0674	4.3	$[M-H]^-$	135.0094, 119.0510	GRR	[28]
127	36.04	Formononetin ^{**}	Flavonoids	$C_{16}H_{12}O_4$	267.0663	267.0671	3.0	$[M-H]^-$	252.0458, 195.0458	ASR	[31]
128	36.32	Senkyunolide F isomer ^{**}	Phthalides	$C_{12}H_{14}O_3$	205.0870	205.0879	4.4	$[M-H]^-$	161.0993	ASR	[20]
129	36.42	2 β -Acetoxy-glycyrrhizin	Saponins	$C_{44}H_{64}O_{18}$	879.4020	879.4034	1.6	$[M-H]^-$	351.0583, 193.0362	GRP	[31]
130	36.61	Tenuifolin	Saponins	$C_{36}H_{56}O_{12}$	679.3699	679.3718	2.8	$[M-H]^-$	455.3180, 425.3074	PRP	[10]
131	36.71	Ginsenoside F3 [*]	Saponins	$C_{41}H_{70}O_{13}$	815.4834	815.4818	-2.0	$[M+COOH]^-$	769.4761, 637.4332, 475.3810, 161.0463	GRR	[42]
132	36.90	20(S)-Ginsenoside Rh1	Saponins	$C_{36}H_{62}O_9$	683.4376	683.4390	2.0	$[M+COOH]^-$	637.4335, 475.3806, 161.0462	GRR	[10]
133	36.90	20(S)-Ginsenoside Rg2	Saponins	$C_{42}H_{72}O_{13}$	829.4955	829.4969	1.7	$[M+COOH]^-$	783.4911, 637.4334, 475.3807, 161.0461	GRR	[35]
134	36.90	22-Hydroxyl-glycyrrhizin	Saponins	$C_{42}H_{62}O_{17}$	837.3914	837.3929	1.8	$[M-H]^-$	661.3603, 485.3294, 351.0583, 193.0362	GRP	[28]
135	37.35	Senkyunolide A isomer [*]	Phthalides	$C_{12}H_{16}O_2$	193.1223	193.1217	-3.1	$[M+H]^+$	147.1163, 175.1113, 137.0594	ASR	[20]
136	37.39	20(R)-Ginsenoside Rg2	Saponins	$C_{42}H_{72}O_{13}$	829.4955	829.4972	2.0	$[M+COOH]^-$	783.4913, 637.4332, 475.3808, 161.0462	GRR	[42]
137	37.68	20(R)-Ginsenoside Rh1	Saponins	$C_{36}H_{62}O_9$	683.4376	683.4393	2.5	$[M+COOH]^-$	637.4336, 475.3807, 161.0463, 1205.5983, 1073.5549,	GRR	[40]
138	37.89	Jujuboside A	Saponins	$C_{58}H_{94}O_{26}$	1251.6015	1251.6036	1.7	$[M+COOH]^-$	749.4461, 455.1431, 179.0564, 161.0463	ZSS	[16]
139	38.73	Ginsenoside Rb1	Saponins	$C_{54}H_{92}O_{23}$	1153.6011	1153.6033	1.9	$[M+COOH]^-$	1107.5962, 945.5427, 783.4889, 621.4396, 459.3908	GRR	[31]
140	39.41	Licorice saponin E2	Saponins	$C_{42}H_{60}O_{16}$	819.3809	819.3819	1.2	$[M-H]^-$	645.3648, 351.0581, 193.0362	GRP	[28]

TABLE 1: Continued.

No.	t_R (min)	Name	Classification	Formula	Theoretical mass (Da)	Measured mass (Da)	Error (ppm)	Precursor ions	Main MS/MS fragment ions	Source	Ref.
141	39.70	Ginsenoside Ro	Saponins	$C_{48}H_{76}O_{19}$	955.4908	955.4918	1.0	[M - H] ⁻	793.4382, 775.4275, 749.451, 731.4392, 523.3806, 455.3537, 613.3755, 569.3857, 179.0569, 119.0355	GRR	[31]
142	39.70	Ginsenoside Rc	Saponins	$C_{53}H_{90}O_{22}$	1123.5906	1123.5918	1.1	[M + COOH] ⁻	1077.5854, 915.5348, 459.3809, 149.0451, 191.0563	GRR	[35]
143	39.79	Licorice saponin G2	Saponins	$C_{42}H_{62}O_{17}$	837.3914	837.3921	0.8	[M - H] ⁻	775.3927, 661.3593, 485.3277, 351.0576, 193.0359	GRP	[28]
144	40.75	Ginsenoside Rb2	Saponins	$C_{53}H_{90}O_{22}$	1123.5906	1123.5908	0.2	[M + COOH] ⁻	1077.5865, 783.4945, 621.4307, 459.3789	GRR	[35]
145	41.14	Ginsenoside Rb3	Saponins	$C_{53}H_{90}O_{22}$	1123.5906	1123.5907	0.1	[M + COOH] ⁻	1077.5871, 783.4955, 621.4311, 459.3792	GRR	[43]
146	41.33	Rhaoglycyrrhizin	Saponins	$C_{48}H_{72}O_{20}$	967.4544	967.4567	2.4	[M - H] ⁻	497.1159, 321.0841, 339.0941 733.4491, 587.39348,	GRP	[10]
147	41.33	Jujuboside B	Saponins	$C_{52}H_{84}O_{21}$	1045.5578	1045.5582	0.4	[M + H] ⁺	533.3637, 455.3536, 437.3432, 369.2802	ZSS	[16]
148	42.59	Chikusetsusaponin IVa	Saponins	$C_{42}H_{66}O_{14}$	793.4380	793.4389	1.1	[M - H] ⁻	631.3854, 455.3525, 569.3834	GRR	[31]
149	42.68	Ginsenoside Rd	Saponins	$C_{48}H_{82}O_{18}$	991.5483	991.5496	1.3	[M + COOH] ⁻	945.5438, 783.4892, 621.438, 459.3857, 179.0563, 161.0457	GRR	[35]
150	42.78	Glycyrrhizic acid	Saponins	$C_{42}H_{62}O_{16}$	821.3965	821.3972	0.9	[M - H] ⁻	759.3961, 645.3648, 469.3324, 351.0572, 193.0356	GRP	[31]
151	43.19	Senkyunolide A isomer*	Phthalides	$C_{12}H_{16}O_2$	193.1223	193.1220	-1.6	[M + H] ⁺	147.1166, 175.1117, 137.0599	ASR	[20]
152	44.03	6,8-Dihydroxy-1,2,4-trimethoxyxanthone**	Xanthenes	$C_{16}H_{14}O_7$	317.0667	317.0675	2.5	[M - H] ⁻	302.0444, 287.0203, 259.0254, 231.0297		[23]
153	44.61	Licorice saponin B2*	Saponins	$C_{42}H_{64}O_{15}$	807.4172	807.4178	0.7	[M - H] ⁻	631.3870, 351.0572, 193.0356	GRP	[31]
154	44.62	Atractylenolide I	Terpene lactones	$C_{15}H_{18}O_2$	231.1379	231.1373	-2.6	[M + H] ⁺	213.1266, 203.1427, 189.0913, 185.1314, 157.1007	ARP	[10]
155	44.70	Atractylenolide III	Terpene lactones	$C_{15}H_{20}O_3$	249.1485	249.1485	-0.1	[M + H] ⁺	231.1405, 213.1207, 185.1277, 175.0688	ARP	[10]
156	45.19	Uralsaponin B	Saponins	$C_{42}H_{62}O_{16}$	821.3965	821.3972	0.9	[M - H] ⁻	759.3961, 645.3648, 469.3324, 351.0572, 193.0356	GRP	[44]
157	46.15	Licorice saponin J2	Saponins	$C_{42}H_{64}O_{16}$	823.4122	823.4131	1.1	[M - H] ⁻	351.0573, 193.0357	GRP	[41]
158	46.25	Ginsenoside Rg6	Saponins	$C_{42}H_{70}O_{12}$	811.4849	811.4852	0.4	[M + COOH] ⁻	765.4808, 619.4225, 205.0721, 161.0459	GRR	[31]
159	46.25	Senegasaponin B*	Saponins	$C_{69}H_{102}O_{31}$	1425.6332	1425.6381	3.4	[M - H] ⁻	1395.6243, 1201.5864, 455.3163, 425.3061	PRP	[29]
160	46.25	Onjisaponin Z*	Saponins	$C_{71}H_{106}O_{32}$	1469.6594	1469.6600	0.4	[M - H] ⁻	1245.6054, 1439.6517, 425.3061, 405.1400, 455.3165	PRP	[29]
161	46.34	Onjisaponin E	Saponins	$C_{71}H_{106}O_{33}$	1485.6544	1485.6545	0.1	[M - H] ⁻	455.3187, 425.3029	PRP	[23]
162	46.53	Onjisaponin Y*	Saponins	$C_{69}H_{102}O_{30}$	1409.6383	1409.6376	-0.5	[M - H] ⁻	1379.6184, 1185.5881, 425.3062, 455.3166	PRP	[29]
163	46.53	Onjisaponin G*	Saponins	$C_{70}H_{104}O_{32}$	1455.6438	1455.6447	0.6	[M - H] ⁻	1425.6341, 993.5078, 425.3062, 455.3166	PRP	[23]

TABLE 1: Continued.

No.	t_R (min)	Name	Classification	Formula	Theoretical mass (Da)	Measured mass (Da)	Error (ppm)	Precursor ions	Main MS/MS fragment ions	Source	Ref.
164	46.63	Ginsenoside Rg4*	Saponins	C ₄₂ H ₇₀ O ₁₂	811.4849	811.4854	0.6	[M + COOH] ⁻	765.4798, 619.4212, 161.0456	GRR	[42]
165	46.82	Ginsenoside Rk3	Saponins	C ₃₆ H ₆₀ O ₈	665.4270	665.4271	0.2	[M + COOH] ⁻	619.4211, 457.3698, 161.0458	GRR	[31]
166	46.82	Licorice saponin C2*	Saponins	C ₄₂ H ₆₂ O ₁₅	805.4016	805.4020	0.5	[M - H] ⁻	645.3637, 351.0575, 193.0356	GRP	[41]
167	46.92	Onjisaponin TH	Saponins	C ₆₅ H ₉₆ O ₂₈	1323.6015	1323.5991	-1.8	[M - H] ⁻	455.3171, 425.3048	PRP	[23]
168	47.11	Ginsenoside Rh4	Saponins	C ₃₆ H ₆₀ O ₈	665.4270	665.4277	1.1	[M + COOH] ⁻	619.4218, 457.3679, 161.0459	GRR	[31]
169	47.40	Zingibrosside R1	Saponins	C ₄₂ H ₆₆ O ₁₄	793.4380	793.4386	0.8	[M - H] ⁻	731.4390, 631.3853, 613.3751, 569.3853, 455.3538	GRR	[42]
170	47.88	Ginsenoside Rg3	Saponins	C ₄₂ H ₇₂ O ₁₃	829.4955	829.4953	-0.2	[M + COOH] ⁻	783.4894, 621.4369, 459.3844, 161.0456	GRR	[31]
171	48.10	E-Ligustilide	Phthalides	C ₁₂ H ₁₄ O ₂	191.1067	191.1060	-3.7	[M + H] ⁺	173.0959, 163.1111, 155.0845, 145.1010	ASR	[20, 33]
172	48.17	Licochalcone A**	Flavonoids	C ₂₁ H ₂₂ O ₄	337.1445	337.1445	0.0	[M - H] ⁻	307.0978, 281.082, 243.104		[31]
173	48.56	Isoglycyrol**	Flavonoids	C ₂₁ H ₁₈ O ₆	365.1031	365.1029	-0.5	[M - H] ⁻	335.0561, 307.0248, 295.0251		[31]
174	49.13	20(S)-Ginsenoside Rs3*	Saponins	C ₄₄ H ₇₄ O ₁₄	871.5061	871.5056	-0.6	[M + COOH] ⁻	825.5012, 783.4903, 621.4387, 459.3845, 765.4792		[35]
175	49.26	Attractylenolide II	Terpene lactones	C ₁₅ H ₂₀ O ₂	233.1536	233.1532	-1.7	[M + H] ⁺	215.1431, 187.1473, 169.1047, 151.0747, 145.1009	ARP	[10]
176	49.33	20(R)-Ginsenoside Rs3**	Saponins	C ₄₄ H ₇₄ O ₁₄	871.5061	871.5074	1.5	[M + COOH] ⁻	825.5021, 783.4910, 621.4384, 459.3875, 765.4807		[35]
177	49.39	Z-Ligustilide	Phthalides	C ₁₂ H ₁₄ O ₂	191.1067	191.1062	-2.6	[M + H] ⁺	173.0956, 163.1112, 155.0847, 145.1010	ASR	[20, 33]
178	50.00	Ginsenoside Rk1*	Saponins	C ₄₂ H ₇₀ O ₁₂	811.4849	811.4850	0.1	[M + COOH] ⁻	765.4802, 603.4275, 161.0458		[31]
179	50.19	Ginsenoside Rg5*	Saponins	C ₄₂ H ₇₀ O ₁₂	811.4849	811.4856	0.9	[M + COOH] ⁻	765.4800, 603.4263, 161.0458		[40]
180	52.21	Glycyrrhetic acid**	Saponins	C ₃₀ H ₄₆ O ₄	469.3323	469.3327	0.9	[M - H] ⁻	425.3406		[31]

*Only detected in Qi-Fu-Yin prescription, not detected in herbs; **detected in Qi-Fu-Yin prescription for the first time.

molecular formula of $C_{29}H_{36}O_{15}$. The detection of fragmentation ions at m/z 461.1667, 443.1555, and 315.1083 suggested the continuous neutral loss of caffeoyl, H_2O , and Rha; therefore, compound 53 was identified as acteoside (Figure S2A). Compounds 86 and 92 produced deprotonated molecular ions $[M - H]^-$ (m/z 651.23), indicating a molecular formula of $C_{31}H_{40}O_{15}$. Fragmentation ions at m/z 505.17 and 475.18 corresponded to their neutral loss of Rha and feruloyl. Compounds 86 and 92 were identified as isomartynoside and martynoside, respectively, based on their retention times (Table 1). Other compounds were also preliminarily characterized according to MS_1/MS_2 data and retention times available in the literature.

3.1.3. ASR. Organic acids and phthalides are the primary components of ASR, and both can be detected in the positive as well as negative ion modes. The loss of acyl residues in the negative ion mode is characteristic of the fragmentation pattern of organic acids. Phthalides were easily detected by the loss of H_2O and CO through ring opening in the positive ion mode. According to the fragmentation rules, 14 organic acids and 13 phthalides were identified.

Compound 5 produced a deprotonated molecular ion $[M - H]^-$ (m/z 353.0878) in the negative ion mode, indicating a molecular formula of $C_{16}H_{18}O_9$. Fragmentation ions at m/z 191.0563 and 161.0245 indicated the presence of caffeoyl, and the m/z values 155.0350 and 127.0400 indicated the continuous loss of CO and CO_2 . Compounds 13 and 15 were isomers of compound 5. Compounds 5, 13, and 15 were identified as 5-caffeoylquinic acid, chlorogenic acid, and 4-caffeoylquinic acid, respectively, according to the retention time (Table 1).

Alkyl phthalides, such as compound 116 (3-n-butylphthalide), showed abundant protonated molecular ions $[M + H]^+$ in the positive ion mode (Table 1). Characteristic fragmentation ions were produced at m/z 173, 155, and 145 because of the continuous or simultaneous neutral loss of H_2O and CO, while hydroxylated phthalides such as compound 55 (senkyunolide I) showed higher intensities at $[M + H - H_2O]^+$ (Table 1).

3.1.4. ARP. Terpenoids and their lactones are the main components of ARP. Terpene lactones were easily detected by the loss of H_2O , CO, and C_nH_{2n} in the positive ion mode. One organic acid and three terpene lactones were identified according to the fragmentation rules.

Compound 175 presented a deprotonated molecular ion $[M - H]^-$ (m/z 233.1532) in the positive ion mode, indicating a molecular formula of $C_{16}H_{18}O_9$. Fragmentation ions at m/z 215.1431 and 187.1473 indicated the continuous neutral loss of H_2O and CO, whereas the m/z values 159.0795, 145.1009, and 131.0848 indicated the continuous neutral loss of C_nH_{2n} ; thus, compound 175 was identified as atractylenolide II (Table 1).

3.1.5. GRP. Flavonoids and saponins are the primary components of GRP. Flavonoids have a cyclohexene

structure, which readily occurred owing to reverse Diels–Alder (RDA) cleavage in the negative ion mode. Except for the aglycones of compounds 77 and 127, all flavonoids were flavonoid glycosides, which were subdivided into O-glycosides and C-glycosides owing to the different bonding types between glycosyl and aglycones (Table 1). The former can only be detected by the loss of different types of glycosyl groups (Glc, Api, and others), whereas the latter can also be detected by the fragments of $C_nH_{2n}O_n$ generated from cross-ring cleavage reactions. Saponins can be easily detected by the characteristic fragments of glucuronic acid residues (GlcA) at m/z 351.05 and 193.03 in the negative ion mode. Seventeen flavonoids, 18 saponins, and 1 organic acid were identified according to the fragmentation rules.

Compound 37 presented an $[M - H]^-$ peak at m/z 563.1408, indicating a molecular formula of $C_{26}H_{28}O_{14}$. Fragmentation ions at the m/z values 503.1197, 473.1098, 443.0992, 413.0882, 383.0778, and 353.0674 indicated the continuous neutral loss of CH_2O (30 Da); therefore, compound 37 was identified as schaftoside, as shown in Figure S2B. Compound 40 was identified as liquiritin using standard solutions, which presented an $[M - H]^-$ peak at m/z 417.1194 and characteristic product ions at m/z 255.0665 with the loss of Glc, and m/z values of 135.0089 and 119.0504 due to RDA cleavage (Table 1). Other flavonoids were identified using data from the literature.

According to the standard solutions, compound 150 was identified as glycyrrhizic acid, which showed $[M - H]^-$ at m/z 821.3972, and m/z 803.3855, 777.4059, and 759.3961 due to the simultaneous loss of CO_2 and H_2O . Fragmentation ions at m/z 645.3648, 469.3324, 351.0572, and 193.0356 indicated that the mother skeleton was connected to two GlcA groups (Table 1). There were some isomers at m/z 821.39, 823.41, and 837.39 that were preliminarily characterized according to their fragmentation rules and retention times in the literature.

3.1.6. ZSS. Flavonoids and saponins are the main components of ZSS. A total of 10 flavonoids, 2 saponins, 9 alkaloids, and 2 organic acids were identified.

Most of the identified flavonoids contained a structure nucleus of spinosin, and a few of them were the common C-glycosyl flavonoids. Fragmentation ions at m/z 327.08 represented the flavonoid base peak of spinosin in the positive ion mode, and m/z 445.11, 427.10, 325.07, and 307.06 were detected in the negative ion mode (Table 1). Compound 47 was identified as spinosin based on a comparison of standard solutions and presented $[M - H]^-$ at m/z 607.1674. Owing to the cross-ring cleavage reaction, characteristic product ions at m/z 487.1252, 367.0823, 337.0722, and 307.0614 were readily observed. In addition, m/z 445.1144 and 427.1039 indicated the neutral loss of Glc and H_2O , as shown in Figure S2C. Other spinosin flavonoids were identified in the same manner. Common C-glycosyl flavonoids also displayed a neutral loss of $C_nH_{2n}O_n$ due to the cross-ring cleavage reaction. Combined with the $[M - H]^-$ peak, compounds 28 and 48 were identified as vicianin II and swertisin, respectively (Table 1).

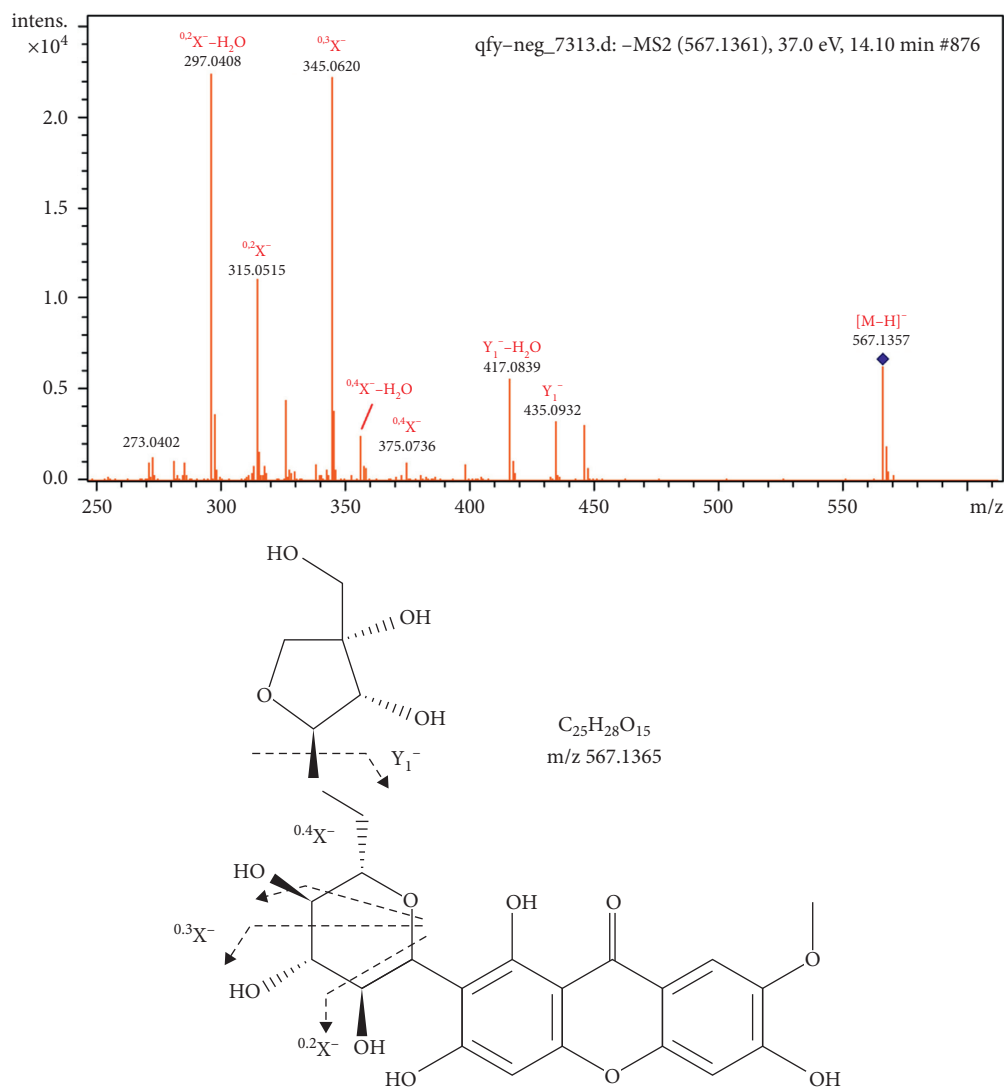


FIGURE 2: MS/MS spectra and the proposed fragmentation pathways of polygalaxanthone III.

A large number of dammarane-type triterpene glycosides, including inner and outer sugar, were detected in ZSS. The inner sugar was usually Ara (132 Da), whereas the outer sugar generally included Xyl (132 Da), Rha (146 Da), or Glc (162 Da). The characteristic aglycone ions and dehydration products of saponin were easily observed at m/z 455.35 and 437.34, respectively.

Alkaloids can only be detected in the positive ion mode. Compounds 12, 23, and 25 yielded $[M]^+$, whereas others produced $[M + H]^+$ peaks (Table 1). According to the MS_1/MS_2 data, eight isoquinoline alkaloids and one cyclopeptide alkaloid were identified.

3.1.7. PRP. The main components of PRP are xanthenes, sucrose esters, oligosaccharide esters, and saponins. Both sucrose esters and xanthenes have low molecular weights, whereas oligosaccharide esters and saponins are larger. Based on the fragmentation characteristics of the different types of components, 16 sucrose esters, 14 oligosaccharide

esters, 11 saponins, 6 xanthenes, and 2 organic acids were identified.

The main characteristic of sugar esters in the negative mode is the neutral loss of acyl (acetyl, feruloyl, p-coumaroyl, sinapoyl, and p-hydroxy benzoyl) residues. For example, compound 90 produced an $[M - H]^-$ ion at m/z 767.2416, which corresponds to the molecular formula of $C_{35}H_{44}O_{19}$. In the MS/MS spectrum, Z_2^- (m/z 529.1567), Z_1^- (m/z 367.1038), $^{0,4}X^-$ (m/z 325.0935), $^{0,2}X^-$ (m/z 265.0721), Y_2^- (m/z 237.0770), Z_0^- (m/z 205.0507), Y_0^- (m/z 223.0613), and $Z_0^- - CH_3$ (m/z 190.0271) ions were formed. The presence of Z_2^- , Y_2^- and Y_0^- , Z_0^- ions indicated the existence of 3,4,5-trimethoxycinnamic acid and sinapoyl, respectively. The presence of Z_2^- , Z_1^- and Z_0^- ions indicated that 3,4,5-trimethoxycinnamic acid and sinapoyl moieties were situated on the glucose and fructose residues, respectively. Therefore, compound 90 was deduced to be tenuifoliside C, as shown in Figure S3. The fragmentation rule of oligosaccharide esters was similar to that of sucrose esters. Compound 119 produced an $[M - H]^-$ ion at m/z 1349.4019,

TABLE 2: Characterization of prototypical components and metabolites in rat plasma and cerebrospinal fluid after oral administration of Qi-Fu-Yin.

No.	t_R (min)	Name	Formula	Theoretical mass (Da)	Measured mass (Da)	Error (ppm)	Precursor ions	Main MS/MS fragment ions	P	CSF
P1	4.17	Sibiricose A5	$C_{22}H_{30}O_{14}$	517.1563	517.1566	0.6	$[M - H]^-$	193.0514, 175.0405, 160.0170 367.1030,	+	
P2	5.13	Sibiricose A1	$C_{23}H_{32}O_{15}$	547.1668	547.1658	-1.8	$[M - H]^-$	223.0627, 205.0508, 190.0274 297.1119,	+	
P3	7.31	Magnoflorine	$C_{20}H_{23}NO_4+$	342.1700	342.1697	-0.8	$[M + H]^+$	282.0888, 265.0843 255.0666,	+	
P4	13.59	Liquiritin	$C_{21}H_{22}O_9$	417.1191	417.1189	-0.5	$[M - H]^-$	135.0091, 119.0508 435.0944, 357.0600,	+	
P5	14.07	Polygalaxanthone III	$C_{25}H_{28}O_{15}$	567.1355	567.1352	-0.5	$[M - H]^-$	345.0606, 315.0522, 297.0395 255.0662,	+	
P6	14.16	Liquiritin apioside	$C_{26}H_{30}O_{13}$	549.1614	549.1609	-0.9	$[M - H]^-$	417.1186, 175.02373, 135.0086, 113.0248 487.1252, 445.1177,	+	
P7	14.85	Spinosin	$C_{28}H_{32}O_{15}$	607.1668	607.1665	-0.5	$[M - H]^-$	367.0823, 337.0722, 307.0614 189.0910,	+	
P8	17.24	Senkyunolide I	$C_{12}H_{16}O_4$	207.1015	207.1012	-1.4	$[M + H - H_2O]^+$	161.1026, 147.0814	+	+
P9	18.77	Senkyunolide H	$C_{12}H_{16}O_4$	207.1015	207.1013	-1.0	$[M + H - H_2O]^+$	-	+	+
P10	18.88	3,6'-Disinapoyl sucrose	$C_{34}H_{42}O_{19}$	753.2248	753.2251	0.4	$[M - H]^-$	547.1668, 529.1565, 265.0748, 223.0595, 205.0540 193.0870,	+	+
P11	19.46	3,4,5-Trimethoxycinnamic acid	$C_{12}H_{14}O_5$	237.0768	237.0766	-0.8	$[M - H]^-$	161.0609, 108.0217 255.0664,	+	
P12	20.90	Isoliquiritin apioside	$C_{26}H_{30}O_{13}$	549.1614	549.1628	2.5	$[M - H]^-$	135.0077, 119.0515 255.0659,	+	
P13	21.29	Isoliquiritin	$C_{21}H_{22}O_9$	417.1191	417.1195	1.0	$[M - H]^-$	135.0089, 119.0499 179.0327, 137.0244	+	
P14	21.58	Tenuifoliside A	$C_{31}H_{38}O_{17}$	681.2036	681.2002	-5.0	$[M - H]^-$	135.0087, 119.0503	+	
P15	22.35	Liquiritigenin	$C_{15}H_{12}O_4$	255.0663	255.0665	0.8	$[M - H]^-$	177.0927, 147.0459	+	
P16	23.69	Senkyunolide D or isomer	$C_{12}H_{14}O_4$	221.0819	221.0823	1.8	$[M - H]^-$	475.3815, 179.0564, 161.0454	+	
P17	24.48	Ginsenoside Rg1	$C_{42}H_{72}O_{14}$	845.4904	845.4900	-0.5	$[M + COOH]^-$		+	

TABLE 2: Continued.

No.	t_R (min)	Name	Formula	Theoretical mass (Da)	Measured mass (Da)	Error (ppm)	Precursor ions	Main MS/MS fragment ions	P	CSF
P18	24.85	Ginsenoside Re	C ₄₈ H ₈₂ O ₁₈	991.5483	991.5436	-4.7	[M + COOH] ⁻	783.4934, 475.3719, 179.0566, 161.0460 177.0925,	+	
P19	26.01	Senkyunolide D or isomer	C ₁₂ H ₁₄ O ₄	221.0819	221.0821	0.9	[M - H] ⁻	147.0453, 134.0374 178.9213,	+	
P20	30.70	Aeginetic acid	C ₁₅ H ₂₄ O ₄	267.1602	267.1608	2.2	[M - H] ⁻	153.0928 455.3189,	+	
P21	32.08	Polygalasaponin XXVIII	C ₅₃ H ₈₄ O ₂₄	1103.5280	1103.5280	0.0	[M - H] ⁻	425.3078 161.0977,	+	
P22	32.66	Senkyunolide F or isomer	C ₁₂ H ₁₄ O ₃	205.0870	205.0872	1.0	[M - H] ⁻	187.9911, 149.0043 171.0768,	+	
P23	32.90	Butylidenephthalide	C ₁₂ H ₁₂ O ₂	189.0910	189.0913	1.6	[M + H] ⁺	161.0935, 143.0845, 117.0676	+	+
P24	33.22	Butylphthalide	C ₁₂ H ₁₄ O ₂	191.1066	191.1064	-1.0	[M + H] ⁺	-	+	+
P25	34.01	Ginsenoside Rf	C ₄₂ H ₇₂ O ₁₄	845.4904	845.4887	-2.0	[M + COOH] ⁻	179.0575, 161.0465	+	
P26	34.38	Senkyunolide A or isomer	C ₁₂ H ₁₆ O ₂	193.1223	193.1228	2.6	[M + H] ⁺	147.1167, 175.1169, 137.0591	+	
P27	35.35	Licorice saponin A3	C ₄₈ H ₇₂ O ₂₁	983.4493	983.4463	-3.1	[M - H] ⁻	351.0583, 193.0364	+	
P28	35.64	Isoliquiritigenin	C ₁₅ H ₁₂ O ₄	255.0663	255.0658	-2.0	[M - H] ⁻	135.0083, 119.0498	+	
P29	35.83	Formononetin	C ₁₆ H ₁₂ O ₄	267.0663	267.0657	-2.2	[M - H] ⁻	-	+	
P30	36.61	Tenuifolin	C ₃₆ H ₅₆ O ₁₂	679.3699	679.3718	2.8	[M - H] ⁻	455.3136, 425.3101	+	+
P31	36.80	22-Hydroxyl-glycyrrhizin	C ₄₂ H ₆₂ O ₁₇	837.3914	837.3894	-2.4	[M - H] ⁻	351.0584, 193.0366 637.4335,	+	
P32	36.89	20(S)-Ginsenoside Rh1	C ₃₆ H ₆₂ O ₉	683.4376	683.4367	-1.3	[M + COOH] ⁻	475.3806, 161.0462 175.1158,	+	+
P33	37.37	Senkyunolide A or isomer	C ₁₂ H ₁₆ O ₂	193.1223	193.1224	0.5	[M + H] ⁺	147.1162, 137.0595	+	
P34	37.66	20(R)-Ginsenoside Rh1	C ₃₆ H ₆₂ O ₉	683.4376	683.4367	-1.3	[M + COOH] ⁻	161.0463 179.0566,	+	+
P35	37.85	Jujuboside A	C ₅₈ H ₉₄ O ₂₆	1251.6015	1251.5971	-3.5	[M + COOH] ⁻	161.0465	+	
P36	38.72	Ginsenoside Rb1	C ₅₄ H ₉₂ O ₂₃	1153.6011	1153.5980	-2.7	[M + COOH] ⁻	1107.5959 793.4379,	+	
P37	39.69	Ginsenoside Ro	C ₄₈ H ₇₆ O ₁₉	955.4908	955.4899	-0.9	[M - H] ⁻	179.0563, 119.0352 459.3809,	+	
P38	39.69	Ginsenoside Rc	C ₅₃ H ₉₀ O ₂₂	1123.5906	1123.5856	-4.5	[M + COOH] ⁻	149.0451, 191.0563 351.056,	+	
P39	39.78	Licorice saponin G2	C ₄₂ H ₆₂ O ₁₇	837.3914	837.3891	-2.7	[M - H] ⁻	193.0351	+	
P40	40.75	Ginsenoside Rb2	C ₅₃ H ₉₀ O ₂₂	1123.5906	1123.5908	0.2	[M + COOH] ⁻	1077.5866	+	
P41	41.32	Rhaoglycyrrhizin	C ₄₈ H ₇₂ O ₂₀	967.4544	967.4506	-3.9	[M - H] ⁻	1077.5859 645.3641,	+	
P42	42.76	Glycyrrhizic acid	C ₄₂ H ₆₂ O ₁₆	821.3965	821.3942	-2.8	[M - H] ⁻	351.0564, 193.0351, 175.0249	+	
P43	42.76	Ginsenoside Rd	C ₄₈ H ₈₂ O ₁₈	991.5483	991.5474	-0.9	[M + COOH] ⁻	179.0564, 161.0456	+	

TABLE 2: Continued.

No.	t_R (min)	Name	Formula	Theoretical mass (Da)	Measured mass (Da)	Error (ppm)	Precursor ions	Main MS/MS fragment ions	P	CSF
P44	44.63	Atractylenolide I	C ₁₅ H ₁₈ O ₂	231.1379	231.1378	-0.4	[M + H] ⁺	-	+	
P45	46.13	Licorice saponin J2	C ₄₂ H ₆₄ O ₁₆	823.4122	823.4091	-3.8	[M - H] ⁻	351.0573, 193.0357	+	
P46	46.90	Ginsenoside Rk3	C ₃₆ H ₆₀ O ₈	665.4270	665.4248	-3.3	[M + COOH] ⁻	161.0449	+	
P47	47.09	Ginsenoside Rh4	C ₃₆ H ₆₀ O ₈	665.4270	665.4258	-1.8	[M + COOH] ⁻	161.0450	+	
P48	47.38	Zingibroside R1	C ₄₂ H ₆₆ O ₁₄	793.4380	793.4374	-0.8	[M - H] ⁻	731.4388, 631.3849 783.4886, 621.4365, 459.3812, 161.0454	+	+
P49	47.86	Ginsenoside Rg3	C ₄₂ H ₇₂ O ₁₃	829.4955	829.4934	-2.5	[M - H] ⁻	459.3812, 161.0454	+	
P50	49.40	Z-Ligustilide	C ₁₂ H ₁₄ O ₂	191.1066	191.1070	2.1	[M + H] ⁺	-	+	
P51	52.30	Glycyrrhetic acid	C ₃₀ H ₄₆ O ₄	469.3323	469.3316	-1.5	[M - H] ⁻	425.3414	+	+
M1	8.78	Ferulic acid-4-sulfate	C ₁₀ H ₁₀ O ₇ S	273.0074	273.0074	0.0	[M - H] ⁻	193.0507, 149.0246	+	
M2	9.45	Ferulic acid-4-sulfate isomer	C ₁₀ H ₁₀ O ₇ S	273.0074	273.0073	-0.4	[M - H] ⁻	193.0504, 149.0245 255.0662,	+	
M3	13.59	Liquiritigenin-7-O-glucuronide	C ₂₁ H ₂₀ O ₁₀	431.0984	431.0977	-1.6	[M - H] ⁻	175.0250, 135.0088	+	+
M4	13.97	Liquiritigenin-4'-O-glucuronide	C ₂₁ H ₂₀ O ₁₀	431.0984	431.0982	-0.5	[M - H] ⁻	255.0662, 175.025, 135.0088	+	+
M5	15.70	Liquiritigenin+2H + sulfate	C ₁₅ H ₁₄ O ₇ S	337.0382	337.0380	-0.6	[M - H] ⁻	257.0824	+	
M6	17.83	Liquiritigenin-4'-O-sulfate	C ₁₅ H ₁₂ O ₇ S	335.0231	335.0225	-1.8	[M - H] ⁻	255.0664, 135.0088, 119.0503	+	
M7	19.36	(Iso) Liquiritigenin+2H + sulfate	C ₁₅ H ₁₄ O ₇ S	337.0382	337.0383	0.3	[M - H] ⁻	257.0823, 151.0401	+	
M8	20.81	(Iso) Liquiritigenin+2H + sulfate	C ₁₅ H ₁₄ O ₇ S	337.0382	337.0385	0.9	[M - H] ⁻	257.0820, 151.0398	+	
M9	21.10	Formononetin-7-O-glucuronide	C ₂₂ H ₂₀ O ₁₀	443.0984	443.0984	0.0	[M - H] ⁻	267.0661, 175.0249, 135.0453	+	
M10	23.12	Isoliquiritigenin-4'-O-glucuronide	C ₂₁ H ₂₀ O ₁₀	431.0984	431.0978	-1.4	[M - H] ⁻	255.0662, 175.0247, 135.0088	+	+
M11	27.07	Isoliquiritigenin+2H + sulfate	C ₁₅ H ₁₄ O ₇ S	337.0382	337.0390	2.4	[M - H] ⁻	257.0821	+	
M12	28.20	Acetylcysteine conjugate of senkyunolide I or senkyunolide H	C ₁₇ H ₂₃ NO ₆ S	370.1324	370.1316	-2.2	[M + H] ⁺	207.1024, 189.0925, 161.0957	+	
M13	29.38	Formononetin-7-O-sulfate	C ₁₆ H ₁₂ O ₇ S	347.0231	347.0230	-0.3	[M - H] ⁻	267.0664, 252.0429 255.0666,	+	
M14	29.67	Isoliquiritigenin-6'-O-sulfate	C ₁₅ H ₁₂ O ₇ S	335.0231	335.0236	1.5	[M - H] ⁻	135.009, 119.0508	+	
M15	38.72	Compound K-H2	C ₃₆ H ₆₀ O ₈	619.4215	619.4193	-3.6	[M - H] ⁻	457.3683, 439.3216 459.3846,	+	
M16	45.27	Compound K	C ₃₆ H ₆₂ O ₈	621.4372	621.4355	-2.7	[M - H] ⁻	179.0559, 161.0453 651.4118,	+	
M17	45.94	Compound K+2O-2H2	C ₃₆ H ₅₈ O ₁₀	665.3906	665.3883	-3.5	[M - H] ⁻	409.2751, 375.2533 605.4042, 491.3720, 175.0237, 113.0242	+	
M18	46.42	Compound K+3O-H2	C ₃₆ H ₅₉ O ₁₁	667.4063	667.4047	-2.4	[M - H] ⁻		+	

TABLE 2: Continued.

No.	t_R (min)	Name	Formula	Theoretical mass (Da)	Measured mass (Da)	Error (ppm)	Precursor ions	Main MS/MS fragment ions	P	CSF
M19	46.90	Compound K+3O-H2	C ₃₆ H ₅₉ O ₁₁	667.4063	667.4042	-3.1	[M-H] ⁻	605.4029, 491.3724, 175.0241, 113.0242 651.4113,	+	
M20	46.99	Compound K+2O-2H2	C ₃₆ H ₅₈ O ₁₀	665.3906	665.3893	-2.0	[M-H] ⁻	409.2746, 375.2527 651.4119,	+	
M21	47.76	Compound K+2O-2H2	C ₃₆ H ₅₈ O ₁₀	665.3906	665.3897	-1.4	[M-H] ⁻	409.2752, 375.2535	+	
M22	48.13	Glycyrrhetic acid-2H	C ₃₀ H ₄₄ O ₄	469.3318	469.3312	-1.3	[M+H] ⁺	451.3203, 423.3243	+	
M23	48.15	Glycyrrhetic acid + O	C ₃₀ H ₄₆ O ₅	485.3272	485.3263	-1.9	[M-H] ⁻	441.3357 491.3368, 473.3269, 443.3161,	+	+
M24	48.34	Compound K+2O-2H2	C ₃₆ H ₅₈ O ₁₀	665.3906	665.3904	-0.3	[M-H] ⁻	193.0352, 175.0246, 113.0242	+	
M25	48.92	Glycyrrhetic acid + O	C ₃₀ H ₄₆ O ₅	485.3272	485.3256	-3.3	[M-H] ⁻	441.3361, 473.3261,	+	+
M26	49.59	Protopanaxadiol+2O + H2	C ₃₀ H ₅₀ O ₅	489.3585	489.3575	-2.0	[M-H] ⁻	445.3677, 375.2896	+	
M27	45.36	Glycyrrhetic acid + O	C ₃₀ H ₄₆ O ₅	485.3272	485.3279	1.4	[M-H] ⁻	441.3383		+

P, plasma; CSF, cerebrospinal fluid; -, not detected +, detected.

corresponding to the molecular formula of C₆₁H₇₄O₃₄, whereas the m/z values 1307.3907 and 163.0409, 145.0304 indicated the presence of acetyl and p-coumaroyl, respectively; thus, it was identified as tenuifolioside H (Table 1). The remaining 15 sucrose esters and 13 oligosaccharide esters were characterized on the basis of fragmentation rules and the literature.

The basic structure of saponins in PRP mainly comprised an aglycone substituted at C-3 with a mono-glucosyl saccharide (A-chain) and at C-28 with a second complex oligosaccharide (B-chain). Saponins produced characteristic fragments at m/z 455 and 425 in the negative ion mode because of the easy elimination of CH₂OH (30 Da) on C-14. For example, compound 107 produced a deprotonated molecular ion [M-H]⁻ (m/z 1103.5328) in the negative ion mode, indicating a molecular formula of C₅₃H₈₄O₂₄. Characteristic fragments were easily observed at m/z 455.3185 [M-H-Glc-H₂O-CO₂-Fuc-Rha-Xyl]⁻ and m/z 425.3075 [M-H-Glc-H₂O-CO₂-Fuc-Rha-Xyl-CH₂O]⁻ in the MS/MS spectrum. Therefore, compound 107 was deduced to be polygalasaponin XXVIII (Table 1). According to the fragmentation rules, the remaining 10 saponins were preliminarily characterized.

Characteristic fragments of C_nH_{2n}O_n were found for xanthenes due to cross-ring cleavage. Compound 41 showed a deprotonated molecular [M-H]⁻ ion at m/z 567.1361, indicating a molecular formula of C₂₅H₂₈O₁₅. In the MS/MS spectrum, fragment ions at m/z 435.0932, 417.0839, 375.0736, 357.0621, 345.0620, 327.0518, 315.0515, and 297.0408 corresponded to Y₁⁻, Y₁⁻-H₂O, ^{0,4}X⁻, ^{0,4}X⁻-H₂O, ^{0,3}X⁻, ^{0,3}X⁻-H₂O, ^{0,2}X⁻, and ^{0,2}X⁻-H₂O, respectively. The

Y₁⁻ ions were generated by the loss of Api. The ^{0,2}X⁻, ^{0,3}X⁻, and ^{0,4}X⁻ ions were observed in the MS/MS spectrum, mainly via the cross-ring cleavage reactions in the Glc residue. Therefore, compound 10 was identified as polygalaxanthone III, as shown in Figure 2.

3.2. Characterizing the Prototype Components in Plasma after Oral Administration of Qi-Fu-Yin. The identification process for the prototype components was similar to that used in vitro. Using the same UPLC-Q-TOF-MS conditions, 51 prototype components were preliminarily identified by comparing the components of Qi-Fu-Yin in vitro, including 24 triterpene saponins, 10 phthalides, 8 flavonoids, 4 sucrose esters, 1 organic acid, 1 alkaloid, 1 xanthone, 1 terpene lactone, and 1 ionone. Among them, 10 components were compared with the reference standards, and others were identified by comparing the retention times, fragmentation pathways, and MS/MS spectra (Table 2, Figure 3).

Some saponins with low molecular weights can be directly absorbed into blood. For example, P53 produced the adduct ion [M+COOH]⁻ (m/z 829.4934) and deprotonated molecular ion [M-H]⁻ (m/z 783.4886), indicating a molecular formula of C₄₂H₇₂O₁₃. Diagnostic ions at m/z 621.4365, 459.3812, and 161.0454 suggested that it was a PPD-type ginsenoside with continuous or simultaneous elimination of Glc moieties. Thus, P53 was assigned to ginsenoside Rg₃ (Figure 4(a)). P41 produced an [M-H]⁻ peak at m/z 837.3891, indicating a molecular formula of C₄₂H₆₂O₁₇. Furthermore, P41 was identified as glycyrrhizin G₂ because of the characteristic fragments of

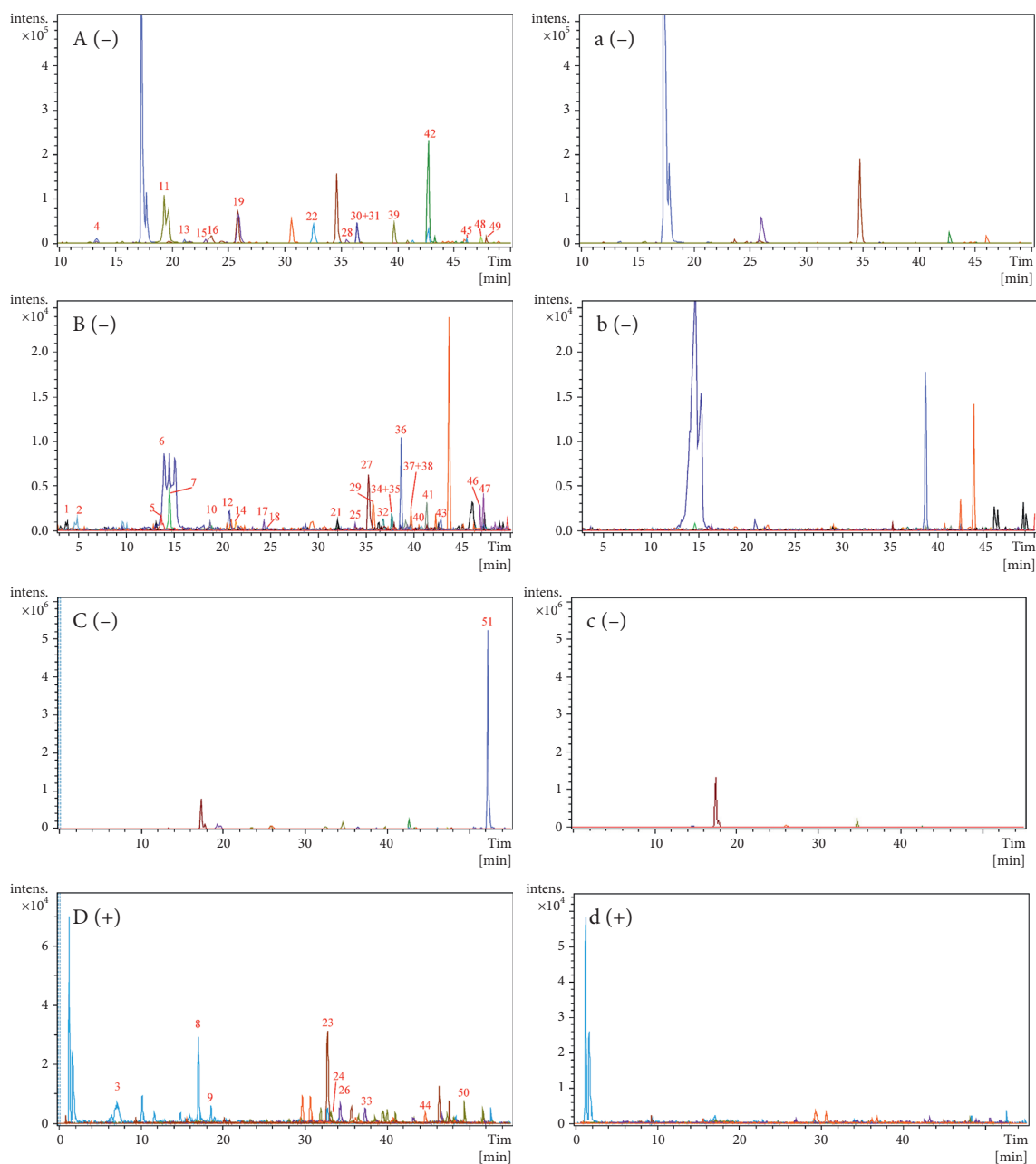


FIGURE 3: Extracted ion chromatograms (EICs) of prototypical components of Qi-Fu-Yin in the dosed and control plasma in the negative and positive ion modes. (A)–(C) Dosed plasma in the negative mode. (a)–(c) Control plasma in the negative mode. (D) Dosed plasma in the positive mode. (d) Control plasma in the positive mode. Because of the presence of many prototype components in rat plasma, they could not be displayed in the same figure and were, therefore, divided into three panels: (A), (B), and (C).

glucuronic acid residues, which were readily detected at m/z 351.056 and 193.0351 in the negative ion mode (Figure 4(b)).

Hydroxylated phthalides showed a higher intensity at $[M+H-H_2O]^+$ and were detected by the loss of H_2O , CO , and C_nH_{2n} through ring opening in the positive ion mode. For example, P10 and P11 produced $[M+H-H_2O]^+$ at m/z 207.10, and the characteristic fragmentation ions at m/z 189.09, 161.10, and 147.08 indicated neutral loss of H_2O , CO , and C_3H_6 . P10 and P11 were identified as senkyunolides I and H, respectively, according to the retention time (Figure S4).

3.3. Characterization of Metabolites in Plasma after Oral Administration of Qi-Fu-Yin. Twenty-six metabolites were preliminarily identified by comparing with data from the metabolite database, mainly including oxidation, reduction, glucuronidation, and sulfation (Table 2, Figure 5). The pathways of some metabolites are shown in Figure 6.

The $[M-H]^-$ ions of M1 and M2 were at m/z 273.00, which showed a mass shift of 79.96 Da (SO_3) from 193.05 [ferulic acid- H] $^-$ and provided the fragment ions at m/z 149.02 [ferulic acid- $H-CO_2$] $^-$. Combined with the predicted chemical formula of $C_{10}H_{10}O_7S$, M1 and M2 were

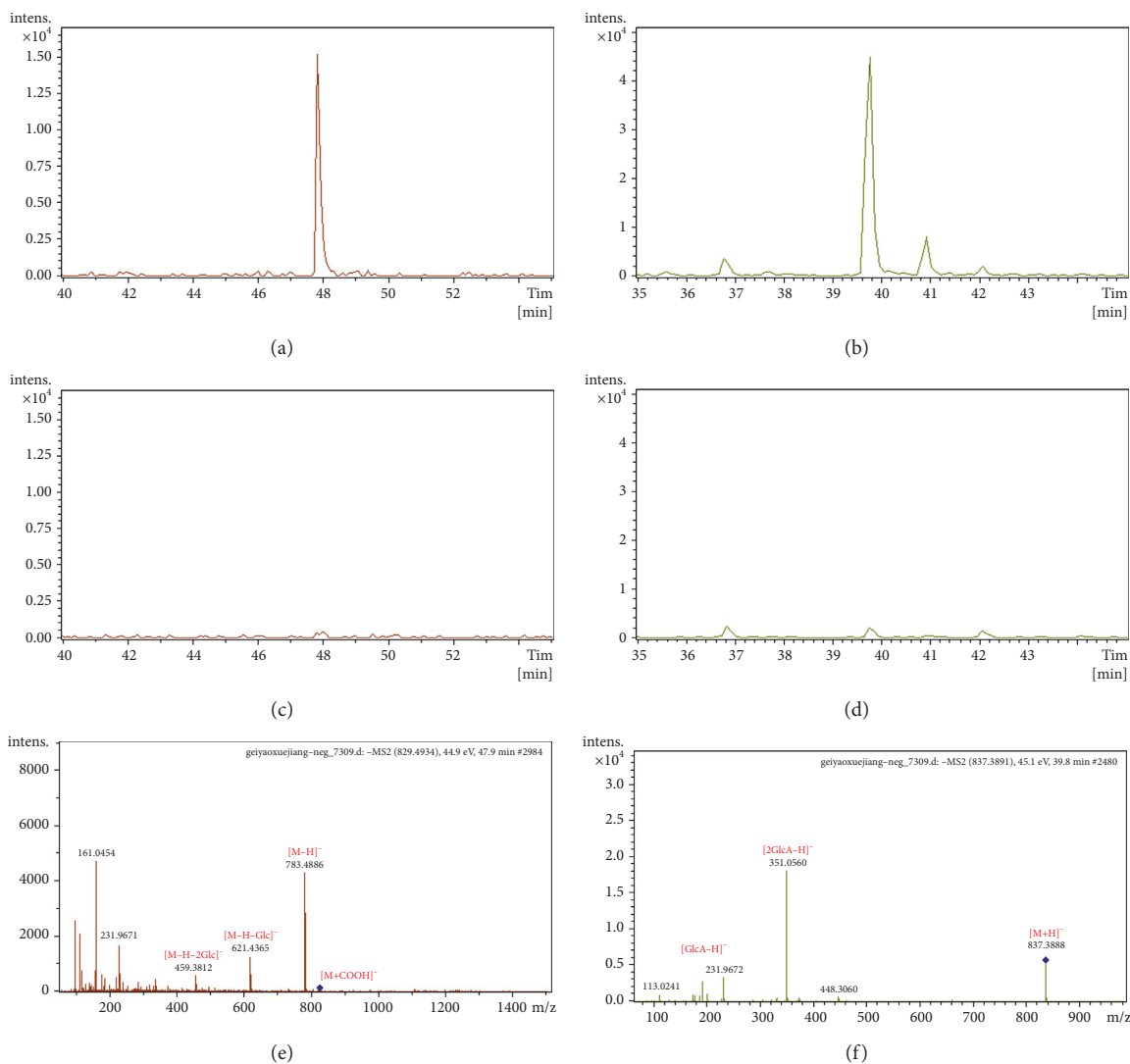


FIGURE 4: EICs and MS/MS spectra of ginsenoside Rg₃ and licorice saponin G₂ in the dosed and control plasma in the negative ion mode. (a) EIC of ginsenoside Rg₃ in the dosed plasma. (b) EIC of licorice saponin G₂ in the dosed plasma. (c) EIC of ginsenoside Rg₃ in the control plasma. (d) EIC of licorice saponin G₂ in the control plasma. (e) MS/MS spectra of ginsenoside Rg₃ in the dosed plasma. (f) MS/MS spectra of licorice saponin G₂ in the dosed plasma.

tentatively deduced to be sulfate conjugates of ferulic acid [36] (Figure 6).

M3, M4, and M10 showed the $[M-H]^-$ ion at m/z 431.10, which was 176.03 Da more than that of isoliquiritigenin. The MS₂ spectra of M3, M4, and M10 all provided fragment ions at m/z 255.07, 175.02, and 135.01, respectively, which suggested the presence of an isoliquiritigenin group. Combining these data with the retention times [46], M3, M4, and M10 were tentatively deduced to be liquiritigenin-7-O-glucuronide, liquiritigenin-4'-O-glucuronide, and isoliquiritigenin-4'-O-glucuronide, respectively (Figure 6).

M6 and M14 showed the $[M-H]^-$ ion at m/z 335.02 (C₁₅H₁₂O₇S), which was 79.96 Da (SO₃) more than that at m/z 255.07. Upon combining data from the retention time and characteristic fragmentation ions at m/z 255.07 and 135.01, M6 and M14 were identified as liquiritigenin-4'-O-sulfate and isoliquiritigenin-6'-O-sulfate, respectively

(Figure 6). Similarly, the $[M-H]^-$ ion of M5, M7, M8, and M11 at m/z 337.04 was approximately 2 Da more than that of M6 and M14. The product ions at m/z 257.08 were also approximately 2 Da more than those at 255.07. Combining these data with the retention time, M5, M7, M8, and M11 were deduced to be hydrogenation and sulfate conjugates of (iso)liquiritigenin (Figure 6).

M9 and M13 produced the same fragment ions at m/z 267.07, which were believed to be metabolites of formononetin; according to the adduct ions of m/z 443.0984 and 347.0230, they were identified as formononetin-7-O-glucuronide and formononetin-7-O-sulfate, respectively (Figure 6).

M12 produced fragmentation ions at m/z 207.1024 $[M+H-145-H_2O]^+$ and 189.0925 $[M+H-145-2H_2O]^+$, which suggested the presence of a phthalide group. Combining these data with the $[M+H]^+$ ion at m/z 370.1316

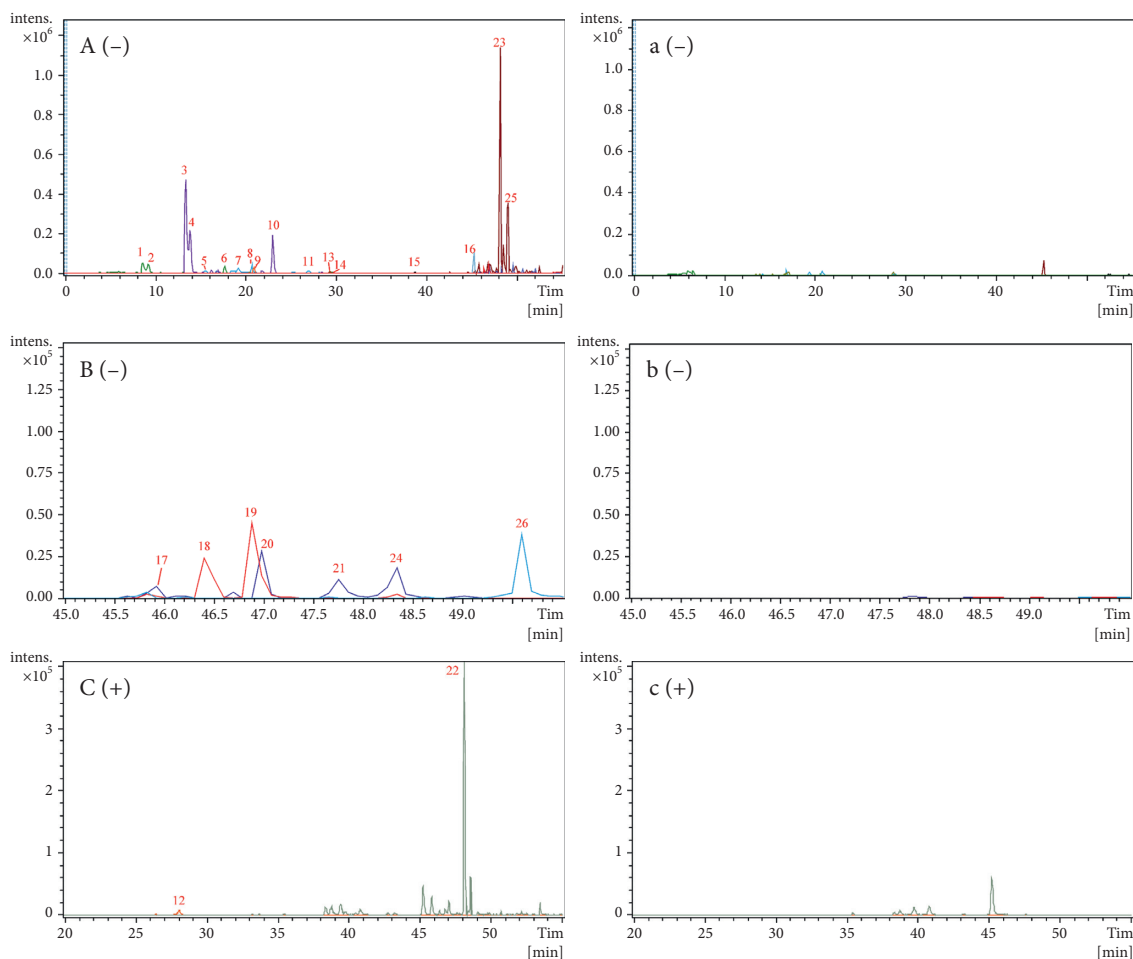


FIGURE 5: EICs of metabolites of Qi-Fu-Yin in the dosed and control plasma in the negative and positive ion modes. (A)-(B) Dosed plasma in the negative mode. (a)-(b) Control plasma in the negative mode. (C) Dosed plasma in the positive mode. (c) Control plasma in the positive mode. Because of the presence of many metabolites in the rat plasma, they cannot be displayed in the same figure and are, therefore, divided into two panels: (A) and (B).

($C_{17}H_{23}NO_6$), M12 was identified as an acetylcysteine conjugate of ligustilide I or H (Table 2).

The fragment ions at m/z 459.3846, 179.0559, and 161.0453 suggested that M16 was a PPD-type ginsenoside. Combining the predicted chemical formula of $C_{36}H_{62}O_8$ and literature [29], M15, M17-21, and M24 were identified as related metabolites of compound K, according to their retention times and chemical formulae [29] (Table 2).

M22 produced fragments of m/z 423.3243 $[M + H - CO_2]^+$ in the positive ion mode, which is in accordance with the fragmentation rules of glycyrrhetic acid. Furthermore, M22 exhibited $[M + H]^+$ at m/z 469.3312, which was determined to be $C_{30}H_{44}O_4$; therefore, M22 was identified as the dehydrogenization of glycyrrhetic acid. Likewise, M23 and M25 produced $[M - H]^-$ ions at m/z 485.3263 and fragments of m/z 441.3357 in the negative ion mode, which represented a neutral loss of CO_2 (44 Da), and were identified as hydroxylate conjugates of glycyrrhetic acid (Table 2).

3.4. Characterization of Prototypical Components and Metabolites in the Cerebrospinal Fluid after Oral

Administration of Qi-Fu-Yin. Using the same UPLC-Q-TOF-MS conditions, 10 prototype components (P8-P10, 23, 24, 30, 32, 34, 48, and 51) and 6 metabolites (M3, 4, 10, 23, 25, and 27) were preliminarily identified by comparing the components of the drugged rat plasma, among which two components were compared with the reference standards, and others were identified by comparing the retention times, fragmentation pathways, and MS/MS spectra (Table 2 and Figure 7).

4. Discussion

In recent years, LC-MS technology has been widely used in the analysis of components of TCM, combining the high separation ability of liquid chromatography with the high sensitivity of mass spectrometry [47, 48]. Up to now, the only research on the identification of components in Qi-Fu-Yin was based on UPLC-Q-TOF-MS in vitro [10]. In this present study, the same 110 components were detected consistent with previous studies [10], and 70 components were preliminarily identified for the first time in vitro (Table 1, Table S1). Among them, forty-four reported

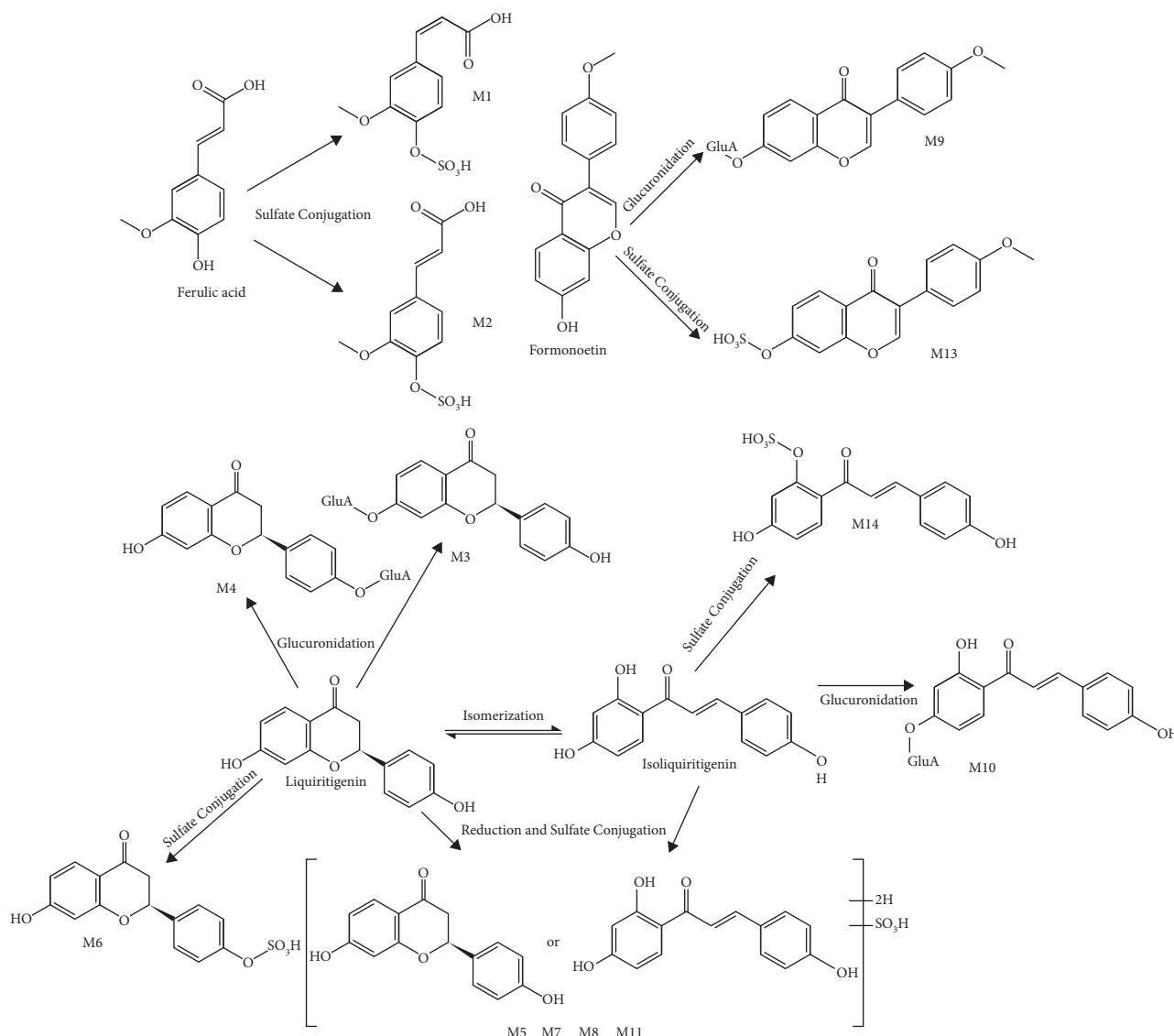


FIGURE 6: Proposed metabolic pathways of some metabolites in rat plasma after oral administration of Qi-Fu-Yin. GluA, glucuronic acid residue.

components [10] were undetected, and 18 of them were lost due to different scanning ranges (Table S1).

Qi-Fu-Yin consists of seven herbs, but there is no research on the similarities and differences of components between them after decocting. For the first time, upon comparing Qi-Fu-Yin with the seven herbs, the categories of chemical components were found to be unanimous, and the number of flavonoids and organic acids in Qi-Fu-Yin was more than the sum of seven herbs; however, the opposite was true for phenylethanoid glycosides (Figure S5). Most of the chemical components could be detected in both, but 9 and 13 chemical components were only detected in the seven herbs and Qi-Fu-Yin, respectively, and the configuration of some components changed (Figure S5, Table 1). This showed that the chemical composition of Qi-Fu-Yin is not a simple addition of compounds in its single herbs.

As far as we know, the prototype components and metabolites of the seven herbs, not Qi-Fu-Yin, in the plasma after

oral administration have been reported. For example, saponins in GRR [49], GRP [46], ZSS [50], flavonoids in GRP [51], ZSS [50], phthalides in ASR [36, 52], sugar esters in PRP [53], phenylethanoid glycosides, and iridoid glycoside in RRP [54] are the main components in plasma after oral administration of herbs. In this research, 51 prototypical components and 26 metabolites of Qi-Fu-Yin, including saponins, phthalides, flavonoids, sucrose esters, organic acids, alkaloids, ionones, terpene lactones, iridoid glycoside, and their derivatives have been tentatively identified in the plasma for the first time.

Similarly, the prototype components and metabolites in the cerebrospinal fluid after oral administration of Qi-Fu-Yin have not been reported. Several research showed that some saponins in GRR [55, 56], GRP [57], and phthalides in ASR [58, 59] can be absorbed into the cerebrospinal fluid. In addition, saponins in GRR [60] and GRP [61], flavonoids in ZSS [62], and sugar esters in PRP [53] have been determined in the brain tissue homogenate. In this research, 10

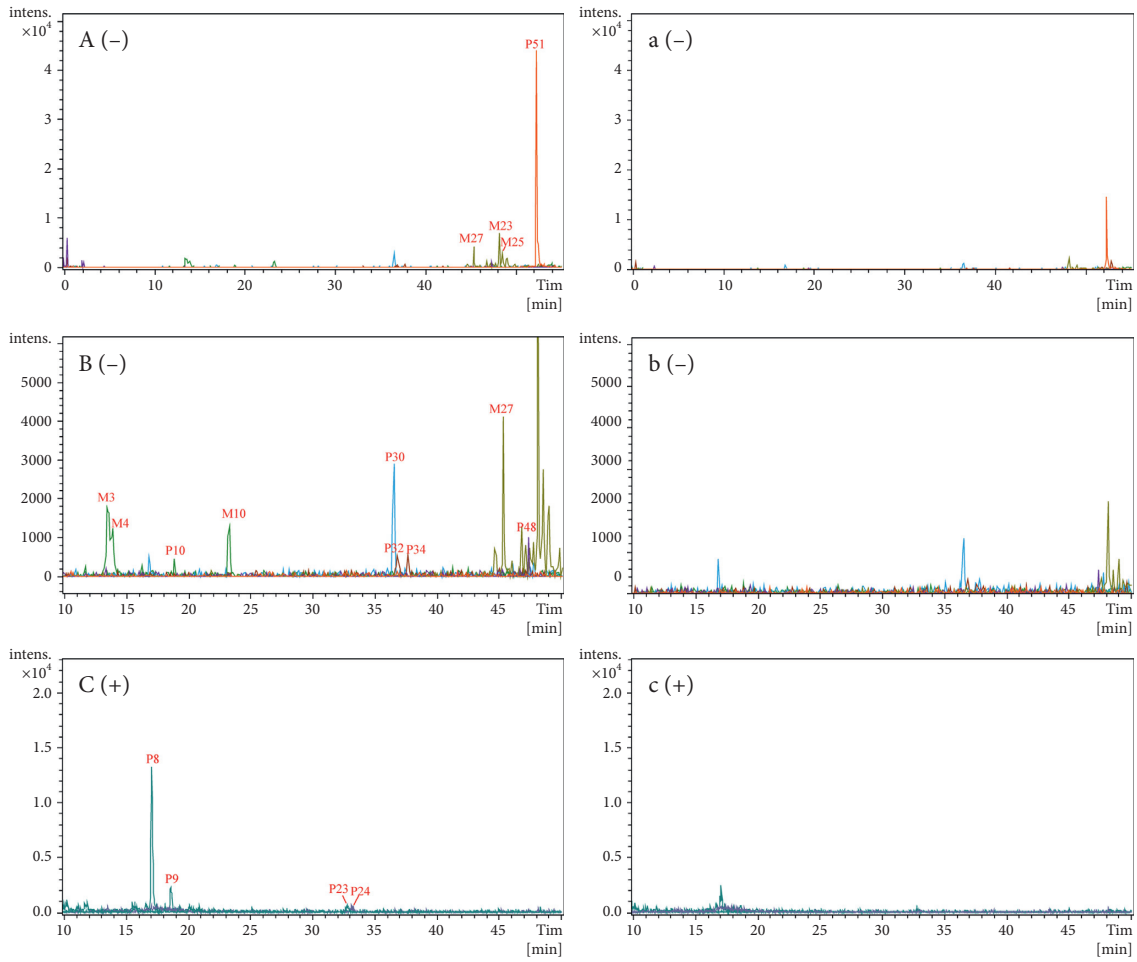


FIGURE 7: EICs of prototypical components and metabolites of Qi-Fu-Yin in the dosed and control cerebrospinal fluid in the negative and positive ion modes. (A)-(B) Dosed cerebrospinal fluid in the negative mode. (a)-(b) Control cerebrospinal fluid in the negative mode. (C) Dosed cerebrospinal fluid in the positive mode. (c) Control cerebrospinal fluid in the positive mode. Because of the presence of many metabolites in the rat cerebrospinal fluid, they cannot be displayed in the same figure and are, therefore, divided into two panels: (A) and (B).

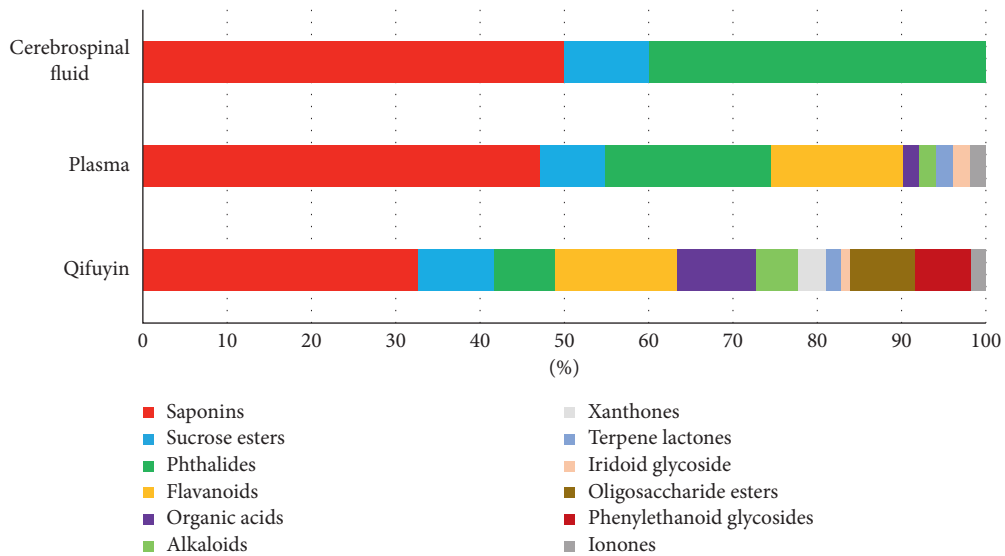


FIGURE 8: Proportion of different types of components in Qi-Fu-Yin, the plasma, and the cerebrospinal fluid.

TABLE 3: Effects of prototype components in the cerebrospinal fluid after oral administration of Qi-Fu-Yin anti-Alzheimer's disease.

Compound	Samples	Biomarkers	Effects	References
3,6'-Disinapoyl sucrose	Glutamate and H ₂ O ₂ -induced SHSY5Y cells	Protein expression of CREB↑ Protein expression of BDNF↑	Neuroprotection	[69]
	Glutamate-induced SHSY5Y cells	mRNA expression of Bax↓ mRNA expression of Bcl-2↑	Antiapoptosis	[70]
Ginsenoside Rh1	Mice (6-month-old)	Number of crosses, time spent in platform quadrant↑ in the Morris water maze test Protein expression of BDNF↑	Neuroprotection	[71]
	IFN-γ-stimulated BV2 cells	Amounts of NO, ROS, and TNF-α↓	Anti-inflammation	[72]
	Scopolamine-induced amnesic mice	Escape latency↓ in the Morris water maze test Activity of SOD and CAT↑	Antioxidative stress	[73]
Butylphthalide	APP/PS1 mice	Escape latency↓, the time spent and travel distance in the target quadrant↑ in the Morris water maze test Protein expression of MAPK↓	Neuroprotection	[74]
	Aβ ₁₋₄₂ -induced SD rats	Amounts of ROS, MDA↓ Activities of SOD, CAT, GSH-Px↑	Antioxidative stress	[75]
Senkyunolide H	phenylpyridinium-induced PC12 cells	Protein expression of Bax and caspase-3↓	Antiapoptosis	[76]
		Amounts of TNF-α, IL-6, and IL-1β↓ mRNA expression of iNOS and COX-2↓ Amount of NO↓	Anti-inflammation Antioxidative stress	[77]
Tenuifolin	Aβ ₁₋₄₂ -induced BV2 cells	Amount of caspase-3↓	Antiapoptosis	[78]
Senkyunolide I	Glutamate-induced Neuro2a cells	Activity of BACE1↓	Neuroprotection	[79]
Glycyrrhetic acid	BACE1 FRET assay			

↓, decrease; ↑, increase; Aβ, amyloid-β; CREB, cyclic AMP response element binding protein; BDNF, brain-derived neurotrophic factor; Bax, Bcl-2 associated X protein; Bcl-2, B cell lymphoma/leukemia-2; NO, nitric oxide; ROS, reactive oxygen species; TNF-α, tumor necrosis factor-α; MDA, malondialdehyde; SOD, superoxide dismutase; CAT, catalase; GSH-Px, glutathione peroxidase; IL-6, interleukin 6; IL-1β, interleukin 1β; iNOS, inducible nitric oxide synthase; COX-2, cyclooxygenase-2; MAPK, mitogen-activated protein kinase; BACE1: β-site APP cleaving enzyme 1.

prototypical components and 6 metabolites were preliminarily characterized in the rat cerebrospinal fluid after oral administration of Qi-Fu-Yin. Among them, butylidenephthalide, butylphthalide, 20(S)-ginsenoside Rh₁, 20(R)-ginsenoside Rh₁, zingibroside R₁, and six other metabolites were detected in the cerebrospinal fluid for the first time. Some prototype components, as saponins, phthalides, and sucrose esters, could be directly absorbed into plasma and cerebrospinal fluid, and phthalides had a higher absorption rate (Figure 8). Some flavonoids, organic acids, alkaloids, xanthenes, terpene lactones, and iridoid glycosides could be absorbed into the plasma, whereas other categories of chemical components were not detected in the plasma and cerebrospinal fluid.

Studies have shown that glycyrrhetic acid [57], 3,6'-disinapoyl sucrose [63], tenuifolin [64], and senkyunolide I and H [65] can be absorbed into cerebrospinal fluid. Some components have been determined in the brain tissue homogenate [66–68], but whether these components can penetrate the BBB is unknown, and they may only exist in the astrocytes and/or vascular endothelial cells constituting the BBB. In this study, 3,6'-disinapoyl sucrose, ginsenoside Rh₁, butylphthalide, glycyrrhetic acid, tenuifolin, and senkyunolide I and H were detected in cerebrospinal fluid. Many studies showed that they had promising effects on

neuroprotection, antiapoptosis, anti-inflammation, or antioxidative stress (Table 3). This suggested that these compounds might be potentially active components of Qi-Fu-Yin for treating AD.

5. Conclusions

In this study, the chemical components of Qi-Fu-Yin in the plasma and cerebrospinal fluid after oral administration of Qi-Fu-Yin were preliminarily characterized using UPLC-Q-TOF-MS. To our knowledge, this is the first systematic investigation of the metabolic profiles of the constituents of Qi-Fu-Yin. In total, 51 prototypical components and 26 metabolites were tentatively identified in plasma. The major phase I metabolic pathway of Qi-Fu-Yin involved hydrogenation and oxidation, whereas that of phase II reactions included sulfate and glucuronic acid conjugation. Furthermore, 10 prototypical components and 6 metabolites, which might be responsible for the potential activity of Qi-Fu-Yin, were preliminarily characterized in the cerebrospinal fluid. This study provides a chemical basis for elucidating the active components of Qi-Fu-Yin that play roles in the treatment of AD and should further motivate research on the mechanisms underlying the anti-AD activity of Qi-Fu-Yin.

Data Availability

The data used to support the findings of this study are included within the article and are available from the corresponding author upon request.

Ethical Approval

All animal procedures were approved by the Shandong University of Traditional Chinese Medicine Institutional Animal Experimentation Committee (SDUTCM20210119001).

Disclosure

Hengyu Li and Hongwei Zhao are co-first authors. Xiaorui Cheng and Jiafeng Wang are conjointly designated as corresponding authors.

Conflicts of Interest

The authors declare that there are no conflicts of interest.

Authors' Contributions

Xiaorui Cheng, Jiafeng Wang initiated and designed the study. Hengyu Li, Hongwei Zhao, and Xiaorui Cheng developed the method and drafted the manuscript. Dongmei Qi and Yong Yang provided experimental platform and equipment. All authors read and approved the final manuscript.

Acknowledgments

The authors would like to thank Shandong Academy of Sciences and Shandong University of Traditional Chinese Medicine Experimental Center for providing experimental platform and equipment and thanks to Xiaoming Wang for guiding this research. This study was supported by Major Basic Research Projects of Natural Science Foundation of Shandong Province (ZR2020ZD17) and Natural Science Foundation of Shandong Province (ZR202103040693, ZR2021QH271).

Supplementary Materials

Figure S1. Base peak chromatograms of Qi-Fu-Yin and seven herbs in the positive (+) and negative (−) ion modes. QFY, Qi-Fu-Yin; GRR, Ginseng Radix et Rhizoma; RRP, Rehmanniae Radix Preparata; ASR, Angelicae Sinensis Radix; ARP, Atractylodis Macrocephala Rhizoma Preparata; GRP, Glycyrrhizae Radix et Rhizoma Preparata Cum Melle; ZSS, Ziziphi Spinosae Semen; PRP, Polygalae Radix Preparata. Figure S2. MS/MS spectra and the proposed fragmentation pathways of acteoside, schaftoside, and spinosyn. (A) MS/MS spectra and the proposed fragmentation pathways for acteoside. (B) MS/MS spectra and the proposed fragmentation pathways of schaftoside. (C) MS/MS spectra and the proposed fragmentation pathways for spinosin. Figure S3. MS/MS spectra and the proposed fragmentation pathways of tenuifoliside C. Figure S4. Extracted ion

chromatograms of senkyunolide I and H in the dosed and control plasma in the negative ion mode. Figure S5. Difference between the chemical components or category and number of chemical components of Qi-Fu-Yin and the seven herbs. (A) Difference between the chemical components of Qi-Fu-Yin and the seven herbs. (B) Difference between the category and number of chemical components of Qi-Fu-Yin and the seven herbs. Table S1. Comparison between the current study and Li's study. (*Supplementary Materials*)

References

- [1] H. Yamashita, K. Ohbuchi, M. Nagino et al., "Comprehensive metabolome analysis for the pharmacological action of inchinkoto, a hepatoprotective herbal medicine," *Metabolomics*, vol. 17, no. 12, p. 106, 2021.
- [2] S. Zeng, Z. Yu, X. Xu et al., "Identification of the active constituents and significant pathways of shen-qi-yi-zhu decoction on antigastric cancer: a network pharmacology research and experimental validation," *Evidence-based Complementary and Alternative Medicine: eCAM*, vol. 2021, Article ID 6642171, 13 pages, 2021.
- [3] W.-Y. Ong, Y.-J. Wu, T. Farooqui, and A. A. Farooqui, "Qi fu yin-a ming dynasty prescription for the treatment of dementia," *Molecular Neurobiology*, vol. 55, no. 9, pp. 7389–7400, 2018.
- [4] G. Wang, "Treatment of 33 cases of Alzheimer's disease with acupuncture combined with Qifuyin," *Zhejiang journal of traditional chinese medicine*, vol. 53, p. 205, 2018.
- [5] G. Zhao and W. Tong, "Clinical efficacy of Qifuyin combined with Donepezil tablets in the treatment of Alzheimer's disease," *China Foreign Medical Treatment*, vol. 33, pp. 145–146, 2014.
- [6] S. Y. Wang, J. P. Liu, W. W. Ji et al., "Qifu-Yin attenuates AGEs-induced Alzheimer-like pathophysiological changes through the RAGE/NF- κ B pathway," *Chinese Journal of Natural Medicines*, vol. 12, pp. 920–928, 2014.
- [7] J. Liu, Q. Wang, Z. Hu, S. Wang, and S. Ma, "Effect the AGEs/RAGE/NF- κ B pathway in Alzheimer's disease model rats of Qifu Yin," *Pharmacology and Clinics of Chinese Materia Medica*, vol. 31, pp. 9–11, 2015.
- [8] G.-H. Xing, C.-R. Lin, X.-J. Zhang, Y.-C. Niu, and X.-Y. Li, "Protective effect of qifu yin on neuronal apoptosis in rats with alzheimer's disease induced by beta-amyloid hippocamp," *Chinese Journal of Experimental Traditional Medical Formulae*, vol. 16, pp. 138–141, 2010.
- [9] G.-H. Xing, C.-R. Lin, N. Hu, Y. Niu, and Y. Sun, "Effect of Qifuyin on ability of learning and memory and expression of somatostatin in Hippocampus on model rats of Alzheimer's disease induced by β -amyloid1-42," *Chinese Journal of Information on TCM*, vol. 17, pp. 34–36, 2010.
- [10] M.-N. Li, X. Dong, W. Gao et al., "Global identification and quantitative analysis of chemical constituents in traditional Chinese medicinal formula Qi-Fu-Yin by ultra-high performance liquid chromatography coupled with mass spectrometry," *Journal of Pharmaceutical and Biomedical Analysis*, vol. 114, pp. 376–389, 2015.
- [11] Y. Yamazaki and T. Kanekiyo, "Blood-brain barrier dysfunction and the pathogenesis of alzheimer's disease," *International Journal of Molecular Sciences*, vol. 18, no. 9, p. 1965, 2017.
- [12] X. Wang, Y. Zhang, H. Niu et al., "Ultra-fast liquid chromatography with tandem mass spectrometry determination

- of eight bioactive components of Kai-Xin-San in rat plasma and its application to a comparative pharmacokinetic study in normal and Alzheimer's disease rats," *Journal of Separation Science*, vol. 40, no. 10, pp. 2131–2140, 2017.
- [13] B. Obermeier, A. Verma, and R. M. Ransohoff, "The blood-brain barrier," *Handbook of Clinical Neurology*, vol. 133, pp. 39–59, 2016.
- [14] G. Serreli, M. R. Naitza, S. Zodio et al., "Ferulic acid metabolites attenuate LPS-induced inflammatory Response in enterocyte-like cells," *Nutrients*, vol. 13, no. 9, p. 3152, 2021.
- [15] J. Li, M. Zhang, Z. Fu et al., "Improvement of the method of extracting rat cerebrospinal fluid by percutaneous puncture," *Chinese Journal of Applied Physiology*, vol. 36, pp. 265–267, 2020.
- [16] D. Wang, Q. Li, R. Liu et al., "Quality control of Semen Ziziphi Spinosae standard decoction based on determination of multi-components using TOF-MS/MS and UPLC-PDA technology," *Journal of Pharmaceutical Analysis*, vol. 9, no. 6, pp. 406–413, 2019.
- [17] S.-L. Li, J.-Z. Song, C.-F. Qiao et al., "A novel strategy to rapidly explore potential chemical markers for the discrimination between raw and processed Radix Rehmanniae by UHPLC-TOFMS with multivariate statistical analysis," *Journal of Pharmaceutical and Biomedical Analysis*, vol. 51, no. 4, pp. 812–823, 2010.
- [18] H.-D. Shen, J.-J. Fang, P.-C. Guo, T.-M. Ding, J.-F. Liu, and X.-P. Ding, "Study of anti-oxidants of Rehmanniae radix and rehmannia radix Praeparata by HPLC-UV-DPPH method," *Chinese Traditional and Herbal Drugs*, vol. 49, pp. 582–588, 2018.
- [19] L.-L. An, K.-M. Li, Q.-Q. He, W.-Z. Yang, G. Liu, and Y.-C. Liu, "Evaluating the quality of Miao medicine *Periploca forrestii* Schltr based on 6 caffeoylquinic acid components combined with stoichiometry," *Chinese Traditional and Herbal Drugs*, vol. 51, pp. 5850–5855, 2020.
- [20] Y. Y. Wu, L. Wang, G. X. Liu, F. Xu, M. Y. Shang, and S. Q. Cai, "Characterization of principal compositions in the roots of *Angelica sinensis* by HPLC-ESI-MSn and chemical comparison of its different parts," *J.Chin. Pharm. Sci.* vol. 23, pp. 393–402, 2014.
- [21] W.-F. Zhong, W.-S. Tong, S.-S. Zhou et al., "Qualitative and quantitative characterization of secondary metabolites and carbohydrates in Bai-Hu-Tang using ultraperformance liquid chromatography coupled with quadrupole time-of-flight mass spectrometry and ultraperformance liquid chromatography coupled with photodiode array detector," *Journal of Food and Drug Analysis*, vol. 25, no. 4, pp. 946–959, 2017.
- [22] F.-x. Zhang, M. Li, L.-r. Qiao et al., "Rapid characterization of Ziziphi Spinosae Semen by UPLC/Qtof MS with novel informatics platform and its application in evaluation of two seeds from *Ziziphus* species," *Journal of Pharmaceutical and Biomedical Analysis*, vol. 122, pp. 59–80, 2016.
- [23] Y. Ling, Z. Li, M. Chen, Z. Sun, M. Fan, and C. Huang, "Analysis and detection of the chemical constituents of Radix Polygalae and their metabolites in rats after oral administration by ultra high-performance liquid chromatography coupled with electrospray ionization quadrupole time-of-flight tandem mass spectrometry," *Journal of Pharmaceutical and Biomedical Analysis*, vol. 85, pp. 1–13, 2013.
- [24] L. Wang, S.-S. Fan, F. Xu, G.-X. Liu, M.-Y. Shang, and S.-Q. Cai, "Analysis of polarity components of *Angelicae Sinensis* Radix and its metabolites in rats by HPLC-MSn," *Chinese Journal of Traditional Chinese Medicine*, vol. 44, pp. 4924–4931, 2019.
- [25] N. Wang, A. Hassan, Y.-M. Jia et al., "Identification of polygalal oligosaccharide esters and their metabolites in rat plasma after oral administration of ethanol extract of Kai Xin San by UHPLC-MS," *Acta Pharmaceutica Sinica*, vol. 52, pp. 1592–1598, 2017.
- [26] Y. Meng, P. Wu, X.-L. Zhang et al., "Rapid identification of chemical components in raw and processed products of Polygalae radix by HPLC/TOF/MS," *Chinese Journal of Experimental Traditional Medical Formulae*, vol. 21, pp. 17–20, 2015.
- [27] Q.-Q. Song, Y.-F. Zhao, N. Zhang et al., "Establishment of HPLC fingerprint of Rehmanniae radix and its HPLC-ESI-MS analysis," *Chinese Traditional and Herbal Drugs*, vol. 47, pp. 4247–4252, 2016.
- [28] W. Xu, M. Huang, H. Li et al., "Chemical profiling and quantification of Gua-Lou-Gui-Zhi decoction by high performance liquid chromatography/quadrupole-time-of-flight mass spectrometry and ultra-performance liquid chromatography/triple quadrupole mass spectrometry," *Journal of Chromatography B*, vol. 986–987, pp. 69–84, 2015.
- [29] G. Feng, *In Vivo and in Vitro Study on Chemical Composition Group of Dingzhi Pills for Alzheimer's Disease Based on Mass Spectrometry*, University of Science and Technology of China, Anhui, China, 2019.
- [30] H.-Y. Li, J.-J. Fang, H.-D. Shen, X.-Q. Zhang, X.-P. Ding, and J.-F. Liu, "Quantity-effect research strategy for comparison of antioxidant activity and quality of Rehmanniae Radix and Rehmannia Radix Praeparata by on-line HPLC-UV-ABTS assay," *BMC Complementary Medicine and Therapies*, vol. 20, no. 1, p. 16, 2020.
- [31] Z. Guan, M. Wang, Y. Cai, H. Yang, M. Zhao, and C. Zhao, "Rapid characterization of the chemical constituents of Sijunzi decoction by UHPLC coupled with Fourier transform ion cyclotron resonance mass spectrometry," *Journal of Chromatography B*, vol. 1086, pp. 11–22, 2018.
- [32] C. Shiwei, Y. fan, Y. Huijuan, and W. Yuefei, "Analysis of chemical constituents in polygala tenuifolia by UPLC/ESI-Q-TOF MS," *Tianjin Journal of Traditional Chinese Medicine*, vol. 35, pp. 60–64, 2018.
- [33] Y.-J. Bai, M. Kong, J.-D. Xu et al., "Effect of different drying methods on the quality of *Angelicae Sinensis* Radix evaluated through simultaneously determining four types of major bioactive components by high performance liquid chromatography photodiode array detector and ultra-high performance liquid chromatography quadrupole time-of-flight mass spectrometry," *Journal of Pharmaceutical and Biomedical Analysis*, vol. 94, pp. 77–83, 2014.
- [34] C.-C. Qu, P. Wu, X.-L. Zhang et al., "Transformation mechanism of oligosaccharides and saponins of prepared Polygalae radix by HPLC-TOF/MS," *Journal of Chinese Medicinal Materials*, vol. 41, pp. 576–580, 2018.
- [35] Z. Liang, Y. Chen, L. Xu et al., "Localization of ginsenosides in the rhizome and root of *Panax ginseng* by laser microdissection and liquid chromatography-quadrupole/time of flight-mass spectrometry," *Journal of Pharmaceutical and Biomedical Analysis*, vol. 105, pp. 121–133, 2015.
- [36] L. Wang, S. Huang, B. Chen et al., "Characterization of the anticoagulative constituents of *Angelicae sinensis* radix and their metabolites in rats by HPLC-DAD-ESI-IT-TOF-MSn," *Planta Medica*, vol. 82, no. 4, pp. 362–370, 2016.

- [37] J. Zhou, G.-R. Shi, Y.-F. Liu, R.-Y. Chen, and D.-Q. Yu, "Five new iridoids from the whole plants of *Rehmannia henryi*," *Journal of Asian Natural Products Research*, vol. 21, no. 8, pp. 727–734, 2019.
- [38] M. He, H. Wu, J. Nie et al., "Accurate recognition and feature qualify for flavonoid extracts from Liang-wai Gan Cao by liquid chromatography-high resolution-mass spectrometry and computational MS/MS fragmentation," *Journal of Pharmaceutical and Biomedical Analysis*, vol. 146, pp. 37–47, 2017.
- [39] Y.-F. Liu, G.-R. Shi, X. Wang et al., "Nine new compounds from the whole plants of *Rehmannia chingii*," *Journal of Asian Natural Products Research*, vol. 18, no. 6, pp. 509–519, 2016.
- [40] W. Wu, L. Sun, Z. Zhang, Y. Guo, and S. Liu, "Profiling and multivariate statistical analysis of *Panax ginseng* based on ultra-high-performance liquid chromatography coupled with quadrupole-time-of-flight mass spectrometry," *Journal of Pharmaceutical and Biomedical Analysis*, vol. 107, pp. 141–150, 2015.
- [41] H. Xiang, L. Zhang, J. Song et al., "The profiling and identification of the absorbed constituents and metabolites of guizhi decoction in rat plasma and urine by rapid resolution liquid chromatography combined with quadrupole-time-of-flight mass spectrometry," *International Journal of Molecular Sciences*, vol. 17, 2016.
- [42] J. Lee, B.-R. Choi, Y.-C. Kim et al., "Comprehensive profiling and quantification of ginsenosides in the root, stem, leaf, and berry of *panax ginseng* by UPLC-QTOF/MS," *Molecules*, vol. 22, no. 12, pp. 2147–2158, 2017.
- [43] H.-P. Wang, Y.-B. Zhang, X.-W. Yang et al., "High-performance liquid chromatography with diode array detector and electrospray ionization ion trap time-of-flight tandem mass spectrometry to evaluate ginseng roots and rhizomes from different regions," *Molecules*, vol. 21, no. 5, pp. 603–616, 2016.
- [44] G.-S. Shan, L.-X. Zhang, Q.-M. Zhao et al., "Metabolomic study of raw and processed *Atractylodes macrocephala* Koidz by LC-MS," *Journal of Pharmaceutical and Biomedical Analysis*, vol. 98, pp. 74–84, 2014.
- [45] L. Zhang, X.-Y. Liu, W. Xu, and X.-W. Yang, "Pharmacokinetics comparison of 15 ginsenosides and 3 aglycones in *Ginseng Radix et Rhizoma* and *Baoyuan* decoction using ultra-fast liquid chromatography coupled with triple quadrupole tandem mass spectrometry," *Phytomedicine*, vol. 59, Article ID 152775, 2019.
- [46] L. Hu, Z. Yao, Z. Qin et al., "In vivo metabolic profiles of Bu-Zhong-Yi-Qi-Tang, a famous traditional Chinese medicine prescription, in rats by ultra-high-performance liquid chromatography coupled with quadrupole time-of-flight tandem mass spectrometry," *Journal of Pharmaceutical and Biomedical Analysis*, vol. 171, pp. 81–98, 2019.
- [47] M. Li, X. Yue, Y. Gao, B. Zhang, C. Yuan, and T. Wu, "Method for rapidly discovering active components in Yupingfeng granules by UPLC-ESI-Q-TOF-MS," *Journal of Mass Spectrometry*, vol. 55, no. 10, Article ID e4627, 2020.
- [48] S. Zhou, Z. Ai, W. Li et al., "Deciphering the pharmacological mechanisms of taohe-chengqi decoction extract against renal fibrosis through integrating network pharmacology and experimental validation in vitro and in vivo," *Frontiers in Pharmacology*, vol. 11, p. 425, 2020.
- [49] Q.-L. Zhou, D.-N. Zhu, Y.-F. Yang, W. Xu, and X.-W. Yang, "Simultaneous quantification of twenty-one ginsenosides and their three aglycones in rat plasma by a developed UFLC-MS/MS assay: application to a pharmacokinetic study of red ginseng," *Journal of Pharmaceutical and Biomedical Analysis*, vol. 137, pp. 1–12, 2017.
- [50] Y. Ren, P. Wang, C. Wu, J. Zhang, and C. Niu, "Identification of the metabolites after oral administration of extract of *ziziphi spinosae* semen to rats or dogs by high-performance liquid chromatography/linear ion trap FTICR hybrid mass spectrometry," *Biomedical Chromatography*, vol. 27, no. 1, pp. 17–26, 2013.
- [51] Z. Zhang, Y. Tang, B. Yu et al., "Chemical composition database establishment and metabolite profiling analysis of Yangyin qingfei decoction," *Biomedical Chromatography: Biomedical Chromatography*, vol. 33, Article ID e4581, 2019.
- [52] Y. Jin, Y. P. Tang, Z. H. Zhu et al., "Pharmacokinetic comparison of seven major bio-active components in normal and blood stasis rats after oral administration of herb pair danggui-honghua by UPLC-TQ/MS," *Molecules*, p. 22, 2017.
- [53] G.-F. Feng, S. Liu, Z.-F. Pi, F.-R. Song, and Z.-Q. Liu, "Comprehensive characterization of in vivo metabolic profile of *Polygalae radix* based on ultra-high-performance liquid chromatography-tandem mass spectrometry," *Journal of Pharmaceutical and Biomedical Analysis*, vol. 165, pp. 173–181, 2019.
- [54] J.-h. Tao, M. Zhao, S. Jiang, W. Zhang, B.-h. Xu, and J.-a. Duan, "UPLC-Q-TOF/MS-based metabolic profiling comparison of four major bioactive components in normal and CKD rat plasma, urine and feces following oral administration of *Cornus officinalis* Sieb and *Rehmannia glutinosa* Libosch herb couple extract," *Journal of Pharmaceutical and Biomedical Analysis*, vol. 161, pp. 254–261, 2018.
- [55] W. Xue, Y. Liu, W.-Y. Qi et al., "Pharmacokinetics of ginsenoside Rg1 in rat medial prefrontal cortex, hippocampus, and lateral ventricle after subcutaneous administration," *Journal of Asian Natural Products Research*, vol. 18, no. 6, pp. 587–595, 2016.
- [56] Y.-N. Zhao, X. Shao, L.-F. Ouyang, L. Chen, and L. Gu, "Qualitative detection of ginsenosides in brain tissues after oral administration of high-purity ginseng total saponins by using polyclonal antibody against ginsenosides," *Chinese Journal of Natural Medicines*, vol. 16, no. 3, pp. 175–183, 2018.
- [57] M. Tabuchi, S. Imamura, Z. Kawakami, Y. Ikarashi, and Y. Kase, "The blood-brain barrier permeability of 18 β -glycyrrhetic acid, a major metabolite of glycyrrhizin in *Glycyrrhiza* root, a constituent of the traditional Japanese medicine yokukansan," *Cellular and Molecular Neurobiology*, vol. 32, no. 7, pp. 1139–1146, 2012.
- [58] Y.-L. Lin, X.-F. Huang, K.-F. Chang, K.-W. Liao, and N.-M. Tsai, "Encapsulated n-butylideneephthalide efficiently crosses the blood-brain barrier and suppresses growth of glioblastoma," *International Journal of Nanomedicine*, vol. 15, pp. 749–760, 2020.
- [59] Q. Zheng, Y. Tang, P.-Y. Hu et al., "The influence and mechanism of ligustilide, senkyunolide I, and senkyunolide A on echinacoside transport through MDCK-MDR1 cells as blood-brain barrier in vitro model," *Phytotherapy Research*, vol. 32, no. 3, pp. 426–435, 2018.
- [60] W. Wei, Z. Li, H. Li et al., "Exploration of tissue distribution of ginsenoside Rg1 by LC-MS/MS and nanospray desorption electrospray ionization mass spectrometry," *Journal of Pharmaceutical and Biomedical Analysis*, vol. 198, Article ID 113999, 2021.
- [61] J. L. Poklis, M. M. Gonek, C. E. Wolf, H. I. Akbarali, and W. L. Dewey, "Analysis of carbenoxolone by ultra-high-performance liquid chromatography tandem mass spectrometry in mouse brain and blood after systemic

- administration,” *Biomedical Chromatography: Biomedical Chromatography*, vol. 33, Article ID e4465, 2019.
- [62] Y. Zhang, T. Zhang, F. Wang, and J. Xie, “Brain tissue distribution of spinosin in rats determined by a new high-performance liquid chromatography-electrospray ionization-mass/mass spectrometry method,” *Journal of Chromatographic Science*, vol. 53, no. 1, pp. 97–103, 2015.
- [63] J. Yang, *Dynamics of the Main Components of Acorus Tatarinowii Schott and Polygala Tenuifolia Willd in Vivo in Rats*, Master, Kunming Medical University, Yunnan, China, 2019.
- [64] Q. Wang, *Pharmacokinetics of Polygala Tenuifolia Saponin Hydrolysate*, Master, Peking Union Medical College, Peking, China, 2012.
- [65] Q. Wang, L. Shen, X. Fang, Y.-L. Hong, Y. Feng, and K.-F. Ruan, “Shift of effective ingredients of Dachuanxiong Decoction along in vitro-plasma-cerebrospinal fluid-brain tissue,” *Chinese Traditional Patent Medicine*, vol. 35, pp. 2364–2371, 2013.
- [66] H.-M. An, M.-N. Li, H. Yang et al., “A validated UHPLC-MS/MS method for pharmacokinetic and brain distribution studies of twenty constituents in rat after oral administration of Jia-Wei-Qi-Fu-Yin,” *Journal of Pharmacy Biomedicine Analytical*, vol. 202, 2021.
- [67] C.-Y. He, S. Wang, Y. Feng et al., “Pharmacokinetics, tissue distribution and metabolism of senkyunolide I, a major bioactive component in *Ligusticum chuanxiong* Hort. (Umbelliferae),” *Journal of Ethnopharmacology*, vol. 142, no. 3, pp. 706–713, 2012.
- [68] B. Ma, X. Li, J. Li et al., “Quantitative analysis of tenuifolin concentrations in rat plasma and tissue using LC-MS/MS: application to pharmacokinetic and tissue distribution study,” *Journal of Pharmaceutical and Biomedical Analysis*, vol. 88, pp. 191–200, 2014.
- [69] Y. Hu, M.-Y. Liu, P. Liu, X. Dong, and A. D. W. Boran, “Neuroprotective effects of 3,6'-disinapoyl sucrose through increased BDNF levels and CREB phosphorylation via the CaMKII and ERK1/2 pathway,” *Journal of Molecular Neuroscience*, vol. 53, no. 4, pp. 600–607, 2014.
- [70] Y. Hu, J. Li, P. Liu et al., “Protection of SH-SY5Y neuronal cells from glutamate-induced apoptosis by 3,6'-disinapoyl sucrose, a bioactive compound isolated from radix polygala,” *Journal of Biomedicine and Biotechnology*, vol. 2012, Article ID 728342, 5 pages, 2012.
- [71] J. Hou, J. Xue, M. Lee, J. Yu, and C. Sung, “Long-term administration of ginsenoside Rh1 enhances learning and memory by promoting cell survival in the mouse hippocampus,” *International Journal of Molecular Medicine*, vol. 33, no. 1, pp. 234–240, 2014.
- [72] J.-S. Jung, D.-H. Kim, and H.-S. Kim, “Ginsenoside Rh1 suppresses inducible nitric oxide synthase gene expression in IFN- γ -stimulated microglia via modulation of JAK/STAT and ERK signaling pathways,” *Biochemical and Biophysical Research Communications*, vol. 397, no. 2, pp. 323–328, 2010.
- [73] C. Lu, Z. Shi, L. Dong et al., “Exploring the effect of ginsenoside Rh1 in a sleep deprivation-induced mouse memory impairment model,” *Phytotherapy Research*, vol. 31, no. 5, pp. 763–770, 2017.
- [74] L. Huang, J. Lan, J. Tang et al., “L-3-n-Butylphthalide improves synaptic and dendritic spine plasticity and ameliorates neurite pathology in Alzheimer’s disease mouse model and cultured hippocampal neurons,” *Molecular Neurobiology*, vol. 58, no. 3, pp. 1260–1274, 2021.
- [75] F.-X. Song, L. Wang, H. Liu, Y.-L. Wang, and Y. Zou, “Brain cell apoptosis inhibition by butylphthalide in Alzheimer’s disease model in rats,” *Experimental and Therapeutic Medicine*, vol. 13, no. 6, pp. 2771–2774, 2017.
- [76] Y. Luo, X. Li, T. Liu et al., “Senkyunolide H protects against MPP⁺-induced apoptosis via the ROS-mediated mitogen-activated protein kinase pathway in PC12 cells,” *Environmental Toxicology and Pharmacology*, vol. 65, pp. 73–81, 2019.
- [77] S. Chen and J. Jia, “Tenuifolin attenuates amyloid- β 42-induced neuroinflammation in microglia through the NF- κ B signaling pathway,” *Journal of Alzheimer’s Disease*, vol. 76, no. 1, pp. 195–205, 2020.
- [78] M. Wang, H. Hayashi, I. Horinokita et al., “Neuroprotective effects of Senkyunolide I against glutamate-induced cells death by attenuating JNK/caspase-3 activation and apoptosis,” *Biomedicine & Pharmacotherapy*, vol. 140, Article ID 111696, 2021.
- [79] A. Wagle, S. H. Seong, B. T. Zhao, M. H. Woo, H. A. Jung, and J. S. Choi, “Comparative study of selective in vitro and in silico BACE1 inhibitory potential of glycyrrhizin together with its metabolites, 18 α - and 18 β -glycyrrhetic acid, isolated from *Hizikia fusiformis*,” *Archives of Pharmacal Research*, vol. 41, no. 4, pp. 409–418, 2018.